The Commonwealth of the Northern Mariana Islands

Final Watershed Plan

APPENDIX C

Engineering Analysis

July 2022

US Army Corps
of Engineers ®
Honolulu District

Table of Contents

List of Figures

List of Tables

1 Study Information

1.1 Purpose & Scope

The purpose of this appendix is to describe the coastal and hydraulic analysis conducted in support of the WA for three islands of the Commonwealth of the Northern Mariana Islands (CNMI), identified as Saipan, Tinian, and Rota. This Engineering Analysis is an addendum to the main planning level study report and incorporates comments received during District Quality Control (DQC), and public review. This report communicates the coastal and hydrologic technical analysis used to support conclusions reached for these watershed assessments. The study intent is to assess the watershed characteristics; identify problems and data gaps; develop, evaluate, and prioritize an array of strategies that include structural and non-structural measures; and identify funding opportunities for Federal and Territorial agencies to support the selected strategy. These watershed assessments incorporate available information from existing data, reports and, on-going efforts from local and federal agencies to provide a suite of recommendations to enhance community resiliency, improve watershed management, and assess the drivers of economic impacts through engagement with the public and other Federal and Territorial agencies.

1.2 Study Location

The CNMI is an unincorporated territory and commonwealth in the United States consisting of 14 islands in the northwestern Pacific Ocean and is located at Latitude 15° 11' 45.03'' and Longitude 145° 45' 00.52" E. The CNMI includes the 14 northernmost islands in the Mariana Archipelago; the southernmost island, Guam, is a separate U.S. territory. Approximately 47,000 people inhabit the islands with the main population centers located on Saipan, Tinian, and Rota, Figure 1, and Figure 2.

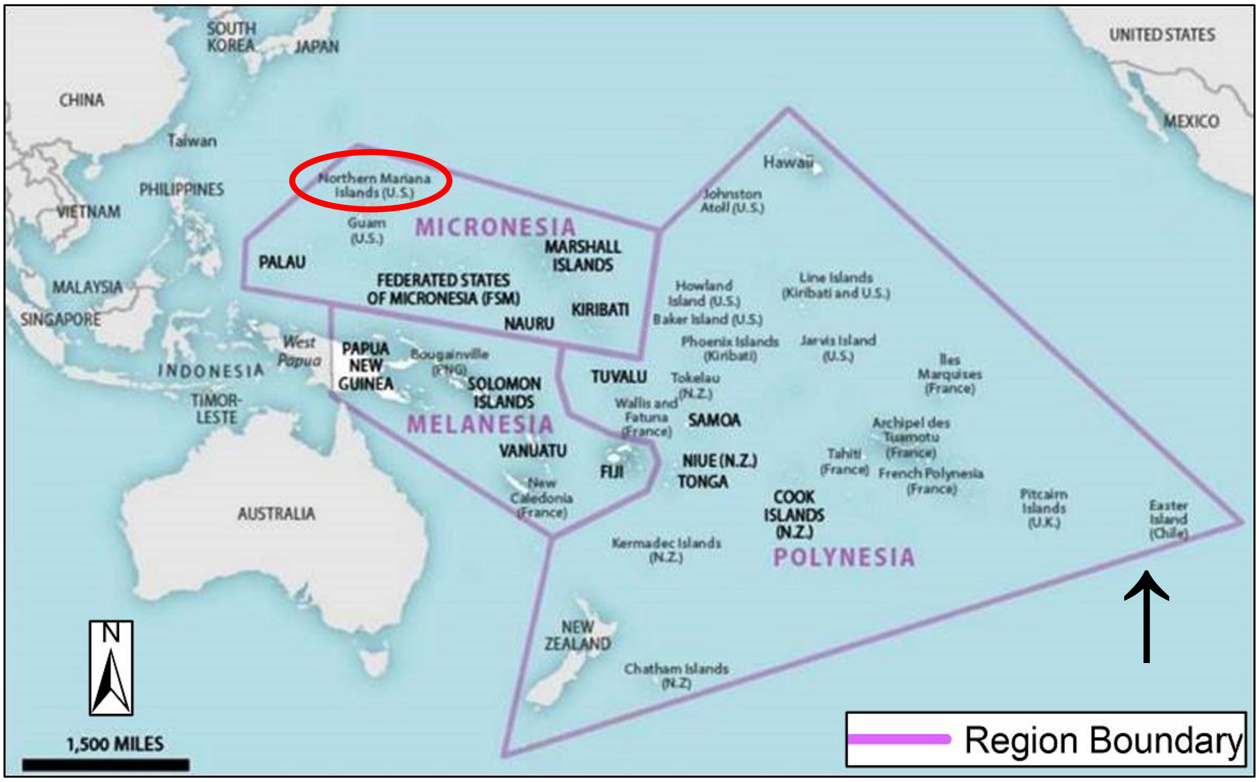

Figure 1. Map of the U.S. Pacific Islands Region

The study area for this watershed assessment focuses on the islands of Saipan, Tinian, and Rota, the most populous and largest islands in CNMI. Saipan has a population of approximately 43,000 and a land area of 46 square miles. Tinian has a population of approximately 2,000 and a land area of 39 square miles. Rota has a population of approximately 2,000 and a land area of 33 square miles. Focusing on these three islands allows the watershed assessment to address the commonwealth-wide need most effectively for community resilience which aims to ensure critical systems are able to resist stressors and rebound quickly from shocks or disturbances.

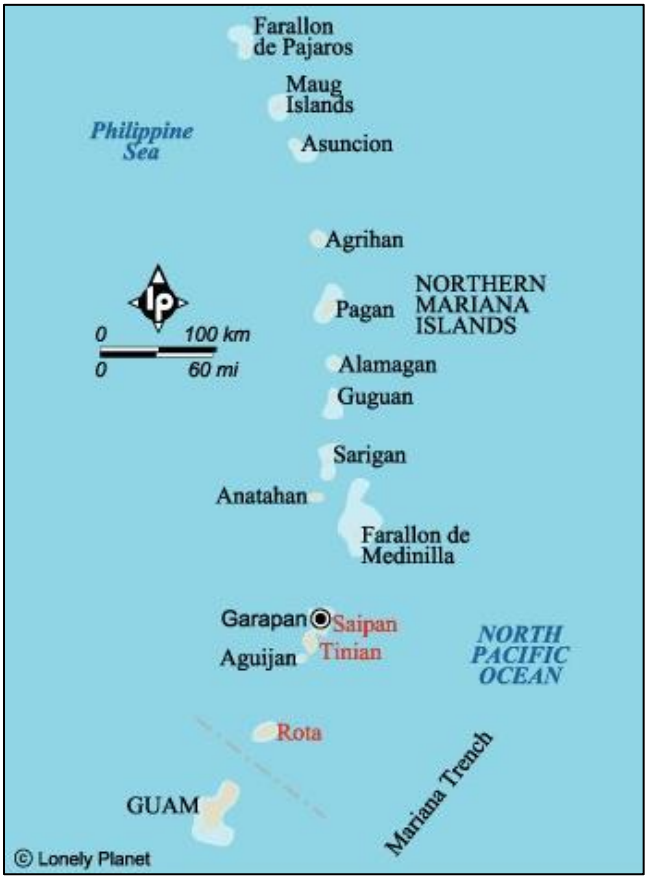

Figure 2. Study Area Comprised of the Islands of Saipan, Tinian, and Rota

2 Existing Conditions

2.1 Datum

The CNMI Vertical Datum of 2003 (NMVD03) is used in the present analysis. The National Geodetic Survey (NGS) published a report labeled the "Development of Comprehensive Geodetic Vertical Datums for the United States Pacific Territories of American Samoa, Guam, and the Northern Marianas" in 2009. This report describes the methodology used by the NGS for the development of Vertical Control Networks in the Northern Marianas with the development of Geodetic control points for Saipan, Tinian, and Rota. This work re-established the definition of the CNMI Vertical Datum of 2003 (NMVD03) and the set of three independent leveling networks on Saipan, Tinian, and Rota. Figure 3. lists the published values for the Northern Marianas Vertical Datum. For more information about this report see the following URL: HTTPS://ngs.noaa.gov/PUBS_LIB/2009DevelopmentOfComprehensiveGeodeticVerticalDatumsForTheUSPacTerritoriesASGUNM)SaLIS.pdf

Northern Marianas Vertical Datum of 2003 (NMVD03)

Northern Marianas Vertical Datum of 2003 (NMVD03) consists of a set of three independent leveling networks on the islands of Rota, Saipan and Tinian (in the Commonwealth of the Northern Mariana Islands). Each of these leveling networks is affixed to a single origin point on their respective islands referenced to the Saipan tide station.

Rota:

- Tide Station & Location = Rota East Harbor, Rota
- PID = **DG4014**
- VM = None
- Bench Mark = Tidal 3
- Ht above LMSL(Meters) = 1.482

Saipan:

- Tide Station & Location = **1633227** -- Tanapag Harbor, Saipan
- PID = **DG3988**
- VM = 16316
- Bench Mark = 163 3227 TIDAL UH-2C
- Ht above LMSL(Meters) = 1.657

Tinian:

- Tide Station & Location = Tinian Harbor, Tinian
- PID = **AA4407**
- VM = None
- Bench Mark = Tidal 1
- Ht above LMSL(Meters) = 2.361

Figure 3. Northern Marianas Vertical Datums

2.2 Climate

2.2.1 Climate

The tropical climate of the Mariana Islands is warm and humid. Mean temperatures vary by as little as eight degrees Fahrenheit (F) throughout the year. The dry season occurs between December through June with a wet and humid season between July through November. August is typically marked with the heaviest precipitation, although precipitation is possible throughout the year. The precipitation trends, as measured by 30-year NOAA climate normal data (NOAA/NWS Saipan, 1991-2020) indicate a slight reduction in mean annual precipitation and a marked increase in annual maximum temperatures (departures from normal). Figure 4 illustrates the increased trend in maximum temperature departures from the mean, which is one representative indicator of climate change (source: http://xmacis.rcc-acis.org/). The X-Axis is time in Years while the Y-Axis is the departure from the mean in degrees Fahrenheit.

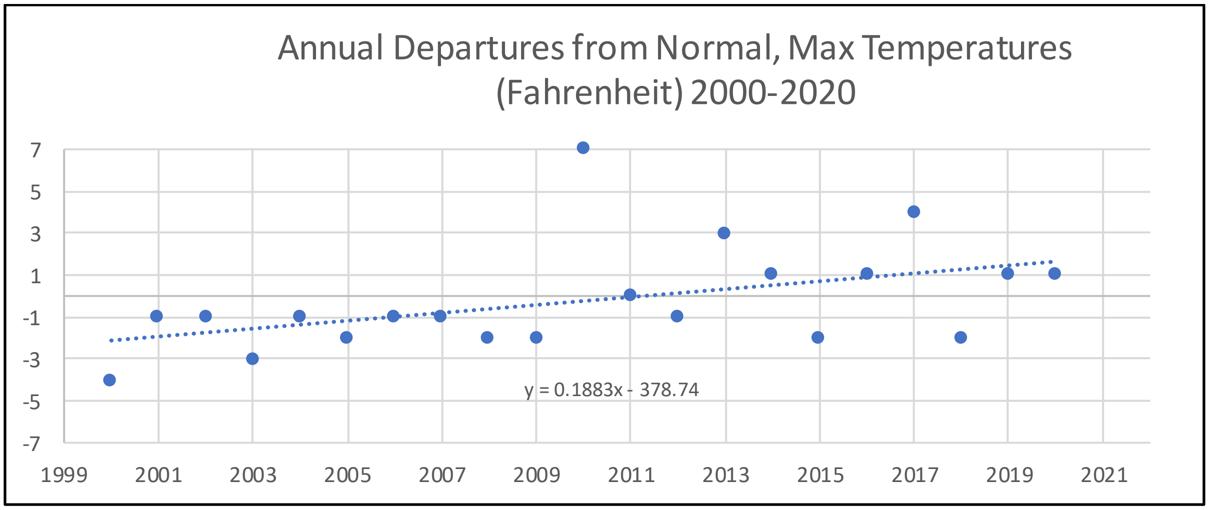

Figure 4. Annual Maximum Temperature Departures from Normal

The annual number of hot days (defined as greater than 88° F) has increased from 5 days to 36 days since 1950 compared to the 1990s. Similarly, a drop in the annual number of cool nights (below 74° F) has dropped from roughly 35 nights to 15 nights over the same period (PIRCA, et al., 2021). The mean annual temperature for Saipan is 81.6° F and the mean annual maximum temperature, measured over the past 20 years, is 92° F. The annual precipitation mean is 69.6 inches (NOAA/NWS, NOWDATA (Tyan, Guam Weather Forecast Office), Data retrieved May 2021. Annual precipitation averages and intensities show little trend over time, but the Mariana Islands are expected to experience greater extremes in rainfall (intensification) as well as droughts in the future (PIRCA et al., 2021) (NOAA[a], 2013). Most of the territory's heavy rainfall, high winds, storm surge, and coastal flooding is brought by tropical storms. The typhoon season occurs July through January, however typhoons have occurred in April and May.

The El Niño Southern Oscillation (ENSO) is a Pacific wide oceanic condition that is quantified by higher water temperatures in the eastern Pacific. ENSO patterns in the Western Pacific are generally the reverse of those conditions that occurs in the Eastern Pacific. When a strong El Niño occurs on the west coast of the United States, cooler water temperatures prevail near the Northern Marianas. Figure 5 presents a summary of conditions experienced during such an event. It is noted that the reverse occurs during a La Niña event in the eastern Pacific, although there is a decreased risk of tropical events near the northern Marianas (IPCC, 2019).

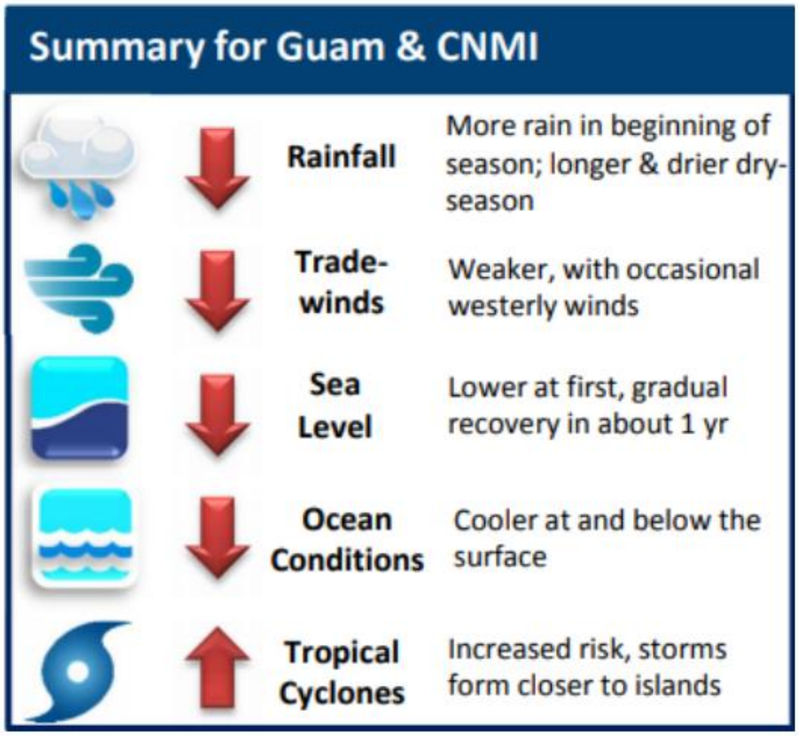

Figure 5. Impacts of El Niño Southern Oscillation on Western Pacific

Climate is strongly correlated to ENSO fluctuations. During El Niño years, easterly trade winds are reduced which allows warmer western Pacific waters and higher sea levels to migrate eastward. This reduces sea levels in the western Pacific, reduces the warm oceanic pool, and is typically followed by drought. El Niño has a wet and dry phase in the western Pacific, which commences with higher rainfall, tropical storm, and typhoon activity, then migrates into drought. The driest year on record over recent decades preceded the strong El Niño event in 1997.

During El Niño events strong typhoons can develop southwest of Hawaii and travel to the Mariana Islands, allowing storms to develop strength. El Niño events are projected to intensify in the Pacific due to climate change (NOAA, 2018). El Niño events not only bring increased tropical storms; they also bring subsequent droughts and are therefore a key driver in weather hazards in the Mariana Islands. Figure 6 illustrates the three ENSO phases of neutral, El Niño (warm ocean temperatures), and La Niña (cooler ocean temperatures) climate conditions. Figure 6 and Figure 7 offers a perspective view of ENSO (source: NOAA, 2018).

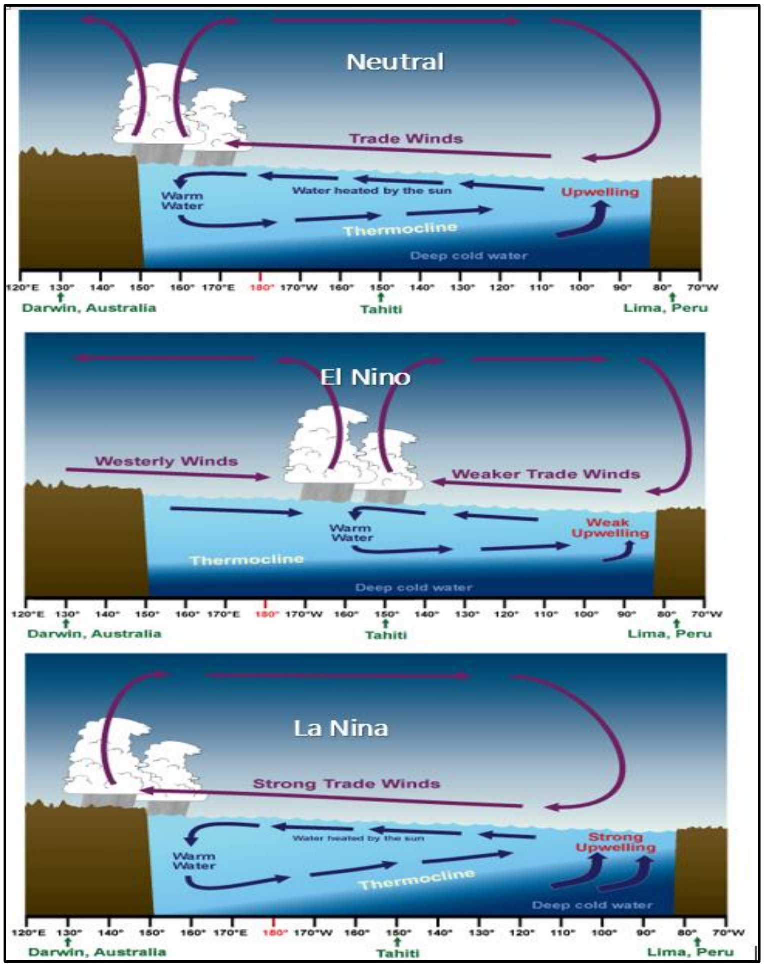

Figure 6. ENSO fluctuations in the Pacific at Equator: Neutral, El Niño, and La Niña

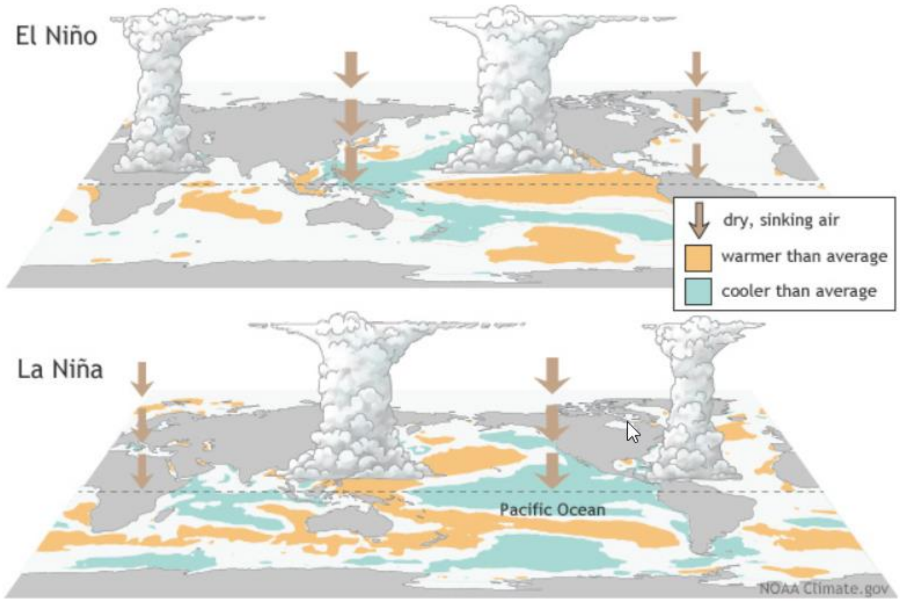

Figure 7. Perspective view of ENSO Fluctuations

2.2.2 Wind

The Mariana Islands have a tropical marine climate and lie within the trade wind latitudes but are also impacted by monsoons. The prevailing winds near the Mariana Islands are easterly trade winds, which approach from the northeast through east-southeast sector.

Trade winds are pronounced during January through May when winds blow from the Northeast more than 90% of the time. Wind directions are far more variable during July through October when tropical cyclones can impact the area. More rain falls in the upper slopes of the islands than in the coastal areas. There are distinct wet and dry seasons, the letter extending from about December to June although the onset of each season is not abruptly marked. Periodic rains can be expected during the dry season. Two main storm systems contribute to the climatic character of the islands; small-scale storms that are locally influenced or large-scale systems such as tropical storms or typhoons. The small-scale systems may only impact areas of a few square miles while larger systems may impact more than a quarter million square miles and can persist for more than a week.

The seasonal trend of wind speed and direction is presented in the box-and-whisker plot in Figure 8. This plot shows the mean value as the star, the median as the red line, the blue box contains the values between the first and third quartile (25th percentile to 75th percentile), the dashed lines to the whisker indicate values between the expected minimum and maximum values and the black crosses indicate the outliers in the dataset.

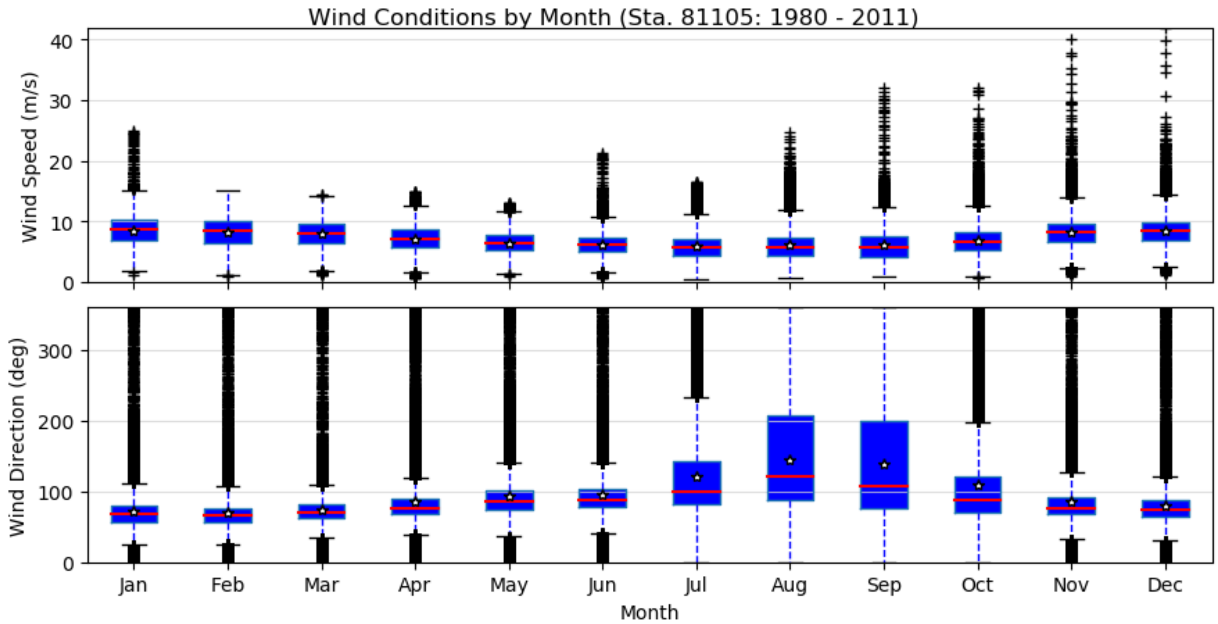

Figure 8. Seasonal Variation of Local Winds (Wave Information Studies 81105)

2.3 Typhoons

A tropical cyclone is a generic term for a warm-core non-frontal cyclonic system over tropical or sub-tropical waters. A tropical storm is a tropical cyclone with maximum sustained winds between 39-73 mph. A typhoon, as they are known in the Western Pacific, is a tropical cyclone with sustained winds greater than 73 mph. Typhoons occur from July to January and are generated very near to the Mariana Islands. Typhoon strength winds can impact the islands within 72 hours after initial storm formation. Wind speeds during typhoons can be 120 mph or greater. The Mariana Islands lie within one of the most active tropical cyclone regions in the world and experience increased risk of storms during El Niño years. Sustained winds of 170 mph and gusts of 200 mph were documented during the October 24-25th 2018 passage of Super Typhoon Yutu through the Mariana Islands. From tropical storm track information, two tropical events impact the Mariana Islands yearly. Figure 9 shows the paths for all tropical events between 1951-2018 passing within 200 nautical miles of Saipan.

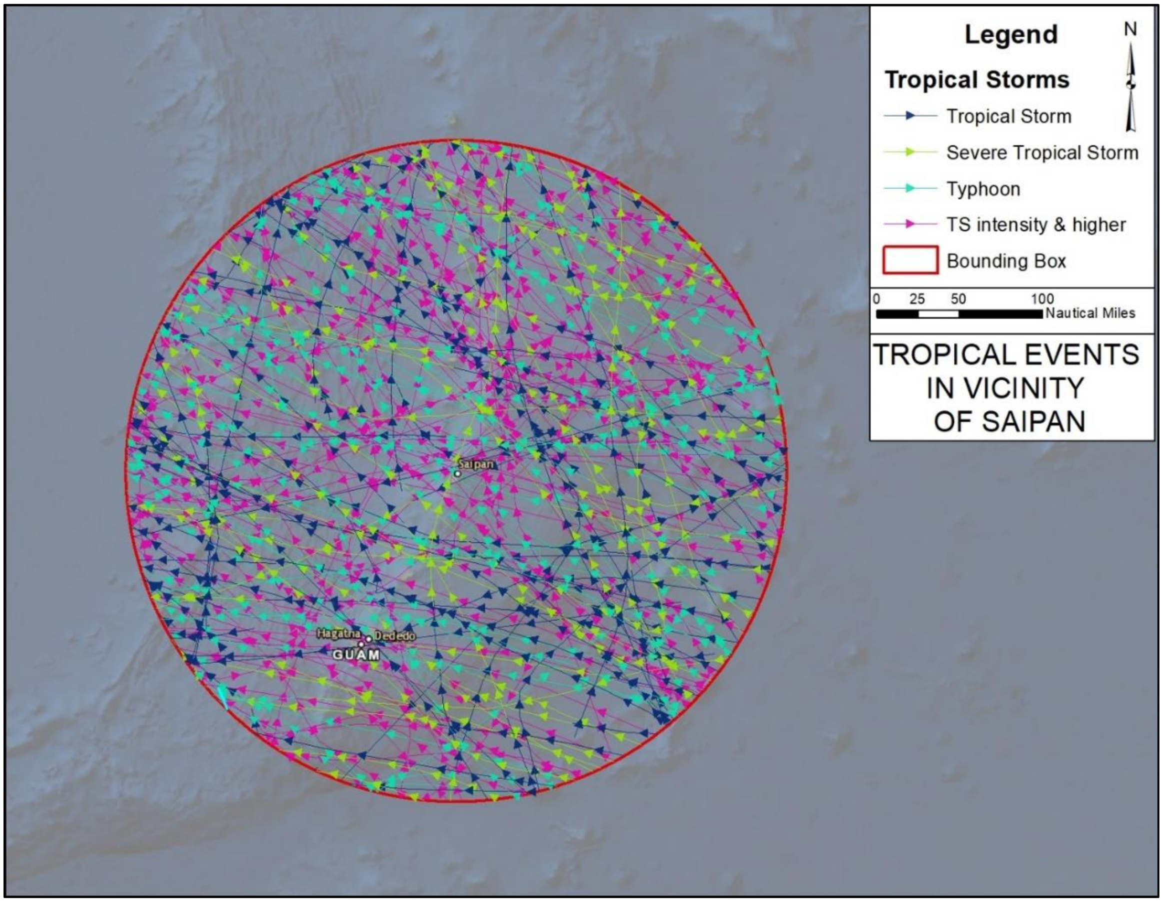

Figure 9. Tropical Storm Tracks from 1951-2018 Passing Within 200 Nautical Miles of Saipan

The effects and duration of typical typhoons are investigated by evaluating the combined storm surge (nontidal residuals) and offshore wave height. It is observed that total storm duration is approximately one day while the peak of the waves lasts approximately 1 to 2 hours as shown in Figure 10 (USACE, 2021). The nontidal residual is highly dependent on both the distance the storm passes from the island and the direction that it passes.

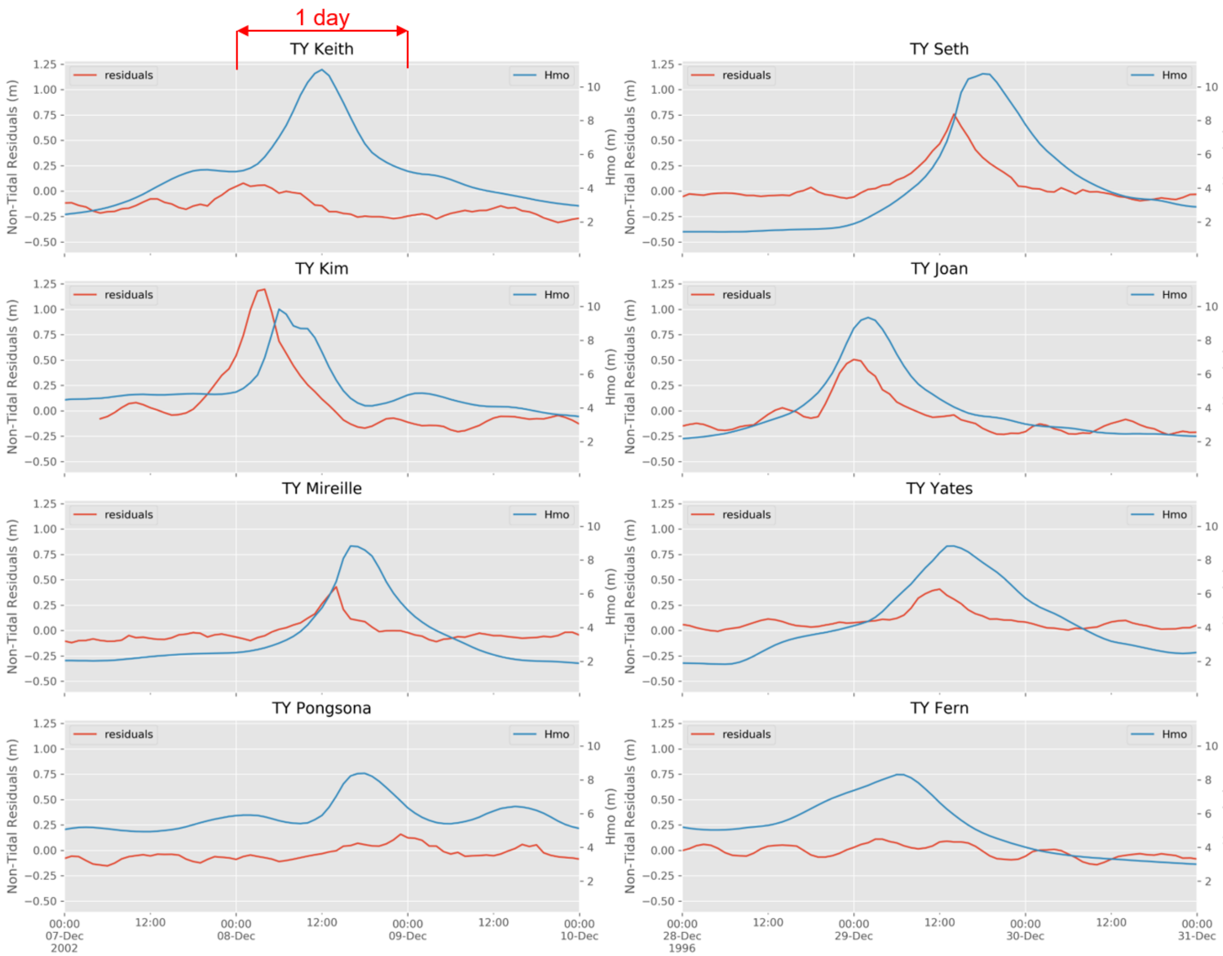

Figure 10. Typhoon Storm Duration Characteristics

2.4 Coastal Waves

There are five distinct wave patterns within the Mariana Islands: local wind (trade wind) generated waves from the east, long period swell energy from the north, local wind generated waves from the north, long period swell energy from the west or southwest and waves associated with tropical cyclones (Fletcher, 2007). The most common condition is trade wind generated wave from the east. Wave Information Studies (WIS) Station ST81420 is approximately 45 nautical miles northwest from Saipan in water depths greater than 10,000 ft. Basic wave statistics developed at this virtual location is shown in Table 1. The wave height climate is graphically shown in the wave rose in Figure 11. Wave Rose for WIS Station ST81420.

Table 1. Wave Statistics for WIS Station ST81420

Statistic	Value
Average wave height:	6.44 ft
Standard deviation of wave height:	2.28 ft
Average wave period:	9.68 sec
Standard deviation of wave period:	1.47 sec
Maximum wave height:	36.15 ft
Period associated w/ max wave height:	14.13 sec
Direction associated w/ max wave height:	92.0 deg
Date associated w/ max wave height:	11/2/1997 12:00
Total number of wave records:	280,511

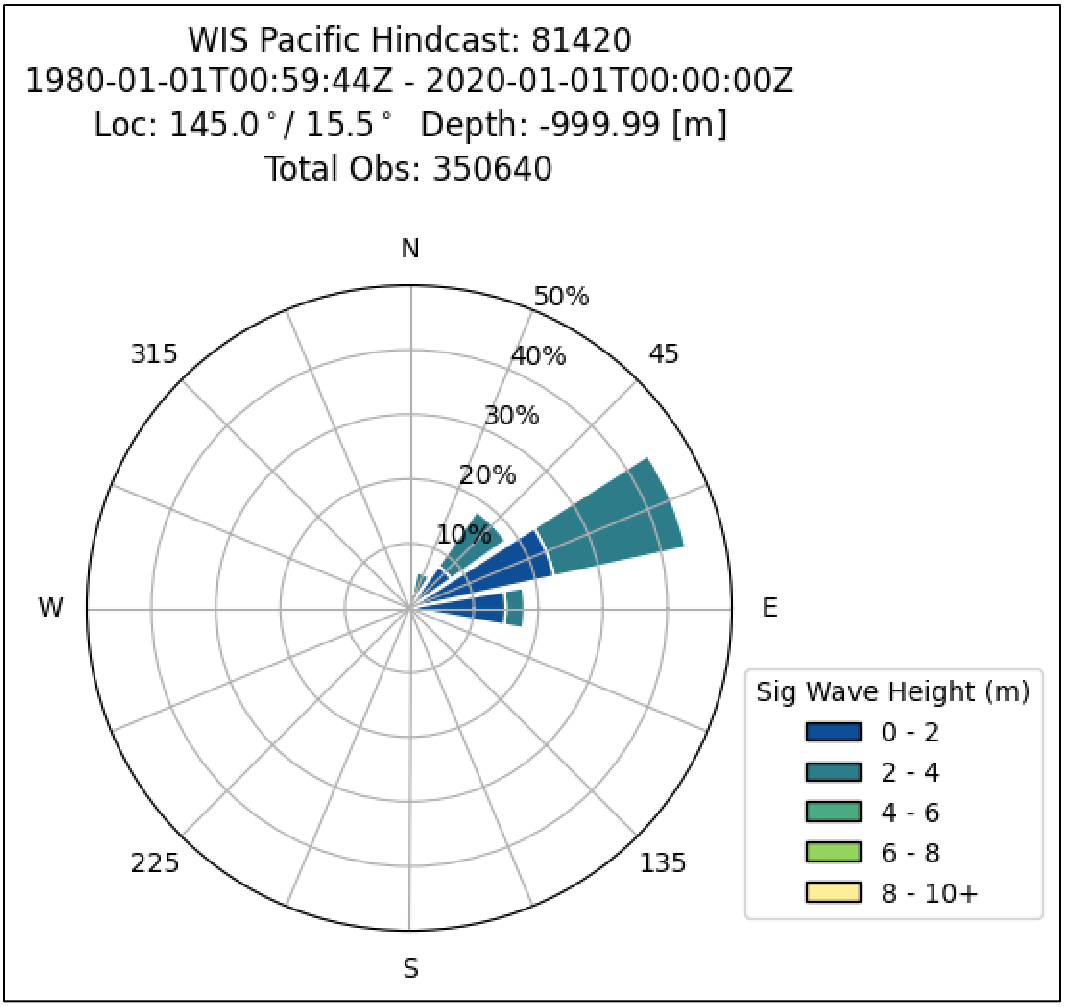

Figure 11. Wave Rose for WIS Station ST81420

2.5 Coastal and Riverine Flooding

The Federal Emergency Management Agency (FEMA) coastal and estuarine flood zones for a 1% annual chance of exceedance (ACE) are shown in Figure 12 through Figure 15. These zones are depicted on a community's Flood Insurance Rate Map (FIRM) or Flood Hazard Boundary Map. Each zone reflects the severity or type of flooding in the area. For areas that are a high risk from flooding from riverine or coastal areas FEMA has defined these zones as described in the Table 2 below.

Table 2. FEMA High Risk Areas- Riverine and Coastal

Zone	Description
A	Riverine areas with a 1% annual chance of flooding and a 26% chance of flooding over the life of a 30-year mortgage. Because detailed analyses are not performed for such areas; no depths or base flood elevations are shown within these zones.
AE	Riverine areas where the base floodplain where base flood elevations are provided. AE Zones are now used on new format FIRMs instead of A1-A30 Zones.
V	Coastal areas with a 1% or greater chance of flooding and an additional hazard associated with storm waves. These areas have a 26% chance of flooding over the life of a 30-year mortgage. No base flood elevations are shown within these zones.
VE	Coastal areas with a 1% or greater chance of flooding and an additional hazard associated with storm waves. These areas have a 26% chance of flooding over the life of a 30-year mortgage. Base flood elevations derived from detailed analyses are shown at selected intervals within these zones.

For more information regarding definitions of FEMA Flood Zone Designations refer to the FEMA Maps Service Center URL: https://msc.fema.gov/portal/home

The inundation maps are expressed as the 1% ACE wave run-up over mean sea level (the equivalent for the CNMI local datum) for coastal (V) (A) and estuarine flood zones. VE or AE zones include base flood elevation (BFE) without the wave run-up calculation (FEMA, April 2006). A zone marked V/VE designates wave run-up that is greater than three feet above a 1% ACE still water elevation (SWEL or BFE). A SWEL assumes a static water line without shoaling or dune effects incorporated in modeling wave run-up. The SWEL is a flood water surface above high tide. An A/AE/AO zone designates a wave run-up depth that is 1-1.5 feet above the SWEL (AO designated sheet flow at 1-1.5 feet of depth). If this zone is adjacent to a V/VE zone it is typically due to raised topography at the location or due to reef or engineered protection. Coastal flooding is escalated by development and impervious roads and infrastructure.

Figure 12. FEMA Flood Zones Southern Saipan

*AE Zone (orange) inland location with hydric soils (wetland)

Figure 13. FEMA Flood Zones Northern Saipan

*****AE Zone (orange) inland location with hydric soils (wetland)

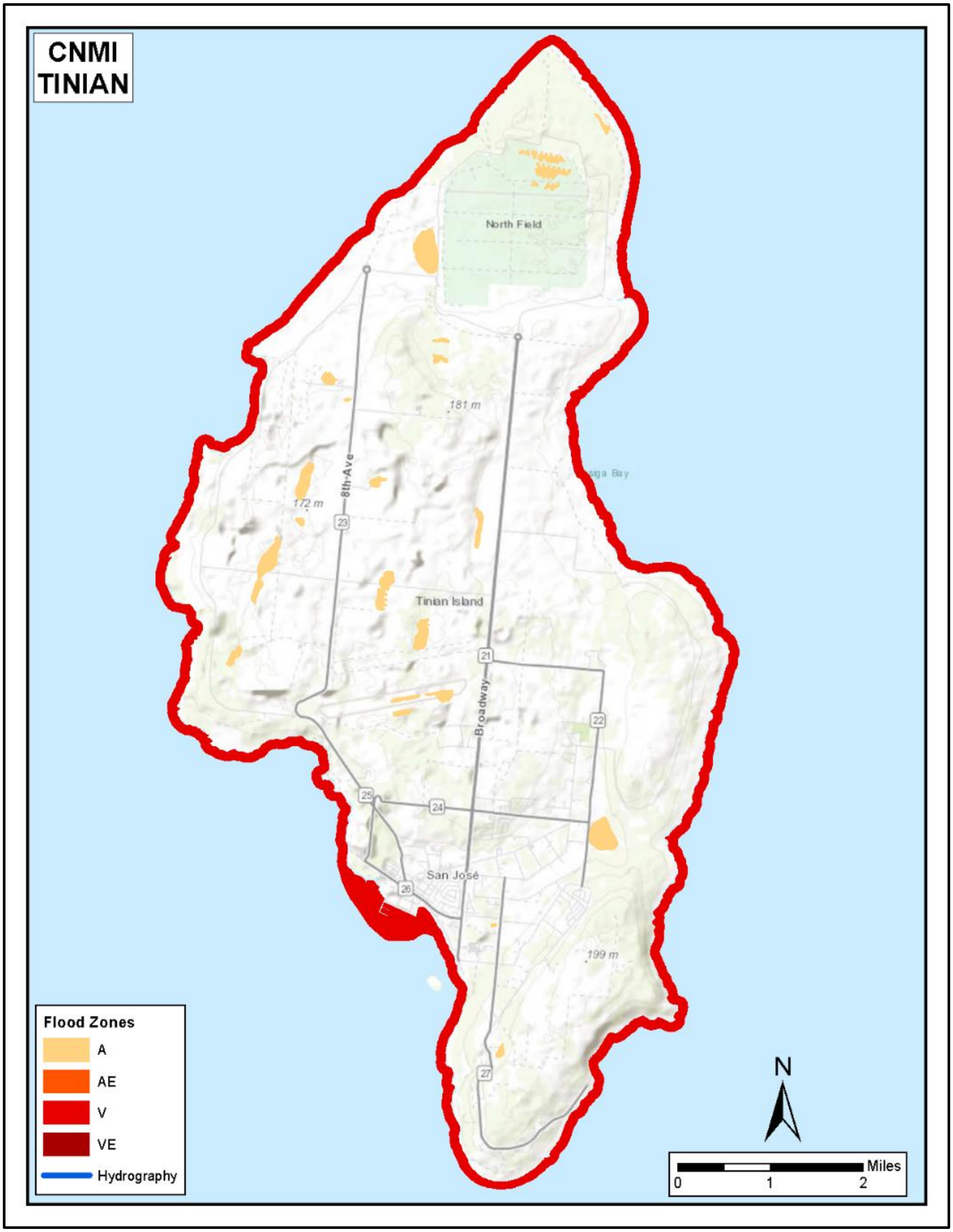

Figure 14. FEMA Flood Zones Tinian

Figure 15. FEMA Flood Zones Rota

Table 3 reflects infrastructure (including critical resources) that fall within the FEMA coastal flood zones and probable maximum tsunami (PMT) zone. Infrastructure inventory was collected in the Economics Section and based off the 2010 Census with building counts in and near the hazard zones.

Table 3. Coastal Flooding - Infrastructure Impacts

FACILITY TYPE	• PMT-TSUNAMI ZONE (OR WITHIN 100 FT) EXISTING CONDITIONS	1% ACE FEMA FLOOD (OR WITHIN 100 FT) EXISTING CONDITIONS	ISLAND
• EVACUATION SHELTER, GARAPAN ELEMENTARY SCHOOL	X	X	SAIPAN
• EVACUATION SHELTER, AGING CENTER	NA*	X	ROTA
• EVACUATION SHELTER, TANAPAG MIDDLE SCHOOL	X		SAIPAN
• EVACUATION SHELTER, WSR ELEMENTARY SCHOOL	X	X	SAIPAN
• EVACUATION SHELTER, MARIANAS HIGH SCHOOL	X	X	SAIPAN
• EVACUATION SHELTER, OLEAI ELEMENTARY SCHOOL	X	X	SAIPAN
• EVACUATION SHELTER, KAGMAN SHELTER AND OLEAI HEAD START	X		SAIPAN
• EVACUATION SHELTER, KOBLERVILL YOUTH CTR	X		SAIPAN

FACILITY TYPE	• PMT-TSUNAMI ZONE (OR WITHIN 100 FT) EXISTING CONDITIONS	1% ACE FEMA FLOOD (OR WITHIN 100 FT) EXISTING CONDITIONS	ISLAND
MEDICAL CENTER, COMMONWEALTH HEALTH CTR CORP MAJOR HEALTH CTR	X		SAIPAN
POWER PLANT, CUC POWER 1 & 4	X	X	SAIPAN
MEDICAL CENTER, ROTA HEALTH CENTER	NA*	X	ROTA
POWER PLANT, CUC POWER	NA*	X	ROTA
GOVERNMENT BLDGs (count)	NA*	0	ROTA
FACILITIES & RESIDENTIAL (count)	NA*	203	ROTA
GOVERNMENT BLDGs (count)	NA*	0	TINIAN
FACILITIES & RESIDENTIAL (count)	NA*	6	TINIAN
GOVERNMENT BLDGs (count)	66	6	SAIPAN
FACILITIES & RESIDENTIAL (count)	3130	981	SAIPAN

NA*= Not Applicable – Facility located out of flood zones.

2.6 Riverine Flooding in Relation to Geology

Saipan, Tinian, and Rota experience storm surge and coastal inundation controlled by terrain. The low-lying elevations have limited shoreline and developable land. The islands are surrounded by fringing reefs and uplifted by tectonic and volcanic activity. The geology the islands predominantly consist of exposed limestone bluffs that overlay a volcanic basement. Limestone weathers through dissolution unlike the erosional and alluvial processes of volcanic soils. Limestone environments are known for limited soil development and poor aquifer environments except where caves and subsurface voids store water. Surface water in karst environments (limestone bedrock with caves, sinkholes, disappearing streams and springs) enter vadose paths (vertical paths from sinkholes and faults) to phreatic storage (saturated zone). Due to the subsurface pirating of surface water runoff, karst terrains are not associated with the same level of flooding as volcanic soils. As observable in the FEMA maps, significant flooding occurs along coastal and low lying urban and impervious zones. Torrential rainfall, however, creates flash flooding and inundation island wide. Streams and flash floods that rapidly run off across impervious zones, fire damaged terrain, and gravel roadways interrupt transportation and convey sediment to near shore habitat. Sedimentation affects reef mortality, shellfish, water quality and clarity, and threaten food security and eco-tourism.

Tinian geology has a 95% carbonate surface with only a few weathered volcanic terrains. Saipan and Rota geology also contain limestone benches with limited detrital and brecciated (broken deposits recemented) calcareous sands, known to retain water. The western coastline of Saipan contains the few marsh and terrace deposits of silty loam and sands. Therefore, coastal flooding is restrained within the narrow shoreline between the limestone bluffs and fringing reefs. For example, Tinian has no perennial streams or recorded streamflow. Runoff is estimated to be 6-12% of rainfall (Cox and Evans, 1956; Belt, Collins Associates, 1983; USGS, 2002). In Saipan, there are also relatively few perennial streams. Talufofo, Sadog Hasngot, and Sadog Denne streams are in the center of the island and drain eastward. As Agatan and Sadog Dogas, part of the Achugao watershed, drain toward the west. Streamflow data (only available for Talufofo) reflect a very limited streamflow, between 1 cubic-feet-per-second (cfs) and 1630 cfs, during the record of 1968 and 1994.

The National Weather Service (NWS) office, located in Tiyan Guam, hosts the only radar for coverage across Guam or CNMI and issues advisories and warnings for the four islands. As with other NWS domains, radar beam blockage from terrain limit accurate data collection. The NWS depends on gage networks for these gaps. There are only three presently active weather gages across the three islands to cover the radar gaps. Saipan has two weather gages, one at the international Airport in the southern island extent, and one on Capitol Hill in central Saipan approximately two miles east of American Memorial Park. Tinian has no active weather gages and Rota has a single weather gage at the Rota International Airport (NOAA NCEI, 2021). Radar scans are typically used for flash flood warnings (a flash flood is a riverine reach with a flood peak under six hours or urban or overland flooding that is a hazard to life safety). Radar is important for flash flooding as the data is scanned every two to six minutes allowing lead time to warn. Automated gage data is updated every 15-60 minutes.

Urban runoff during heavy rainfall events creates flooding in these low-lying areas with poor storm water management and proximity to storm surge and high tides. On Rota, many of the feeder roads joining Route 10 and Route 100 into Songsong are gravel roads that suffer high erosion rates during rainfall (CNMI, 2018). During dry conditions dust is carried into the near shore habitat as well as during rainfall runoff. The territory is working towards paving the roads.

Compound flooding refers to a phenomenon in which two or more flooding sources occur simultaneously or subsequently within a short period of time. In terms of coastal flooding, a compound flooding event is flooding caused by the interaction of the open ocean, atmosphere, and watersheds. As CNMI is made up from a portion of a submerged mountain range and has very steep terrain and the alluvial fans are very short we believe there are insignificant areas where the phenomenon of compound flooding exists.

2.7 Riverine Erosion

Limestone bedrock dominates the CNMI terrain. Karst topography (limestone geology with sinkholes, caves, and disappearing streams) is well known for thin soils and non-cohesive geomorphology. Calcareous sands and alluvium constitute most of the low-lying shoreline soils. Some regions with clays exist, however soils in CNMI are moderately to highly erodible based on the thin and non-cohesive soil types and steep slopes. The following watersheds are noted as moderately erodible (USDA, 2021) and are depicted in Figure 16 and Figure 17. Note that the Kagman and Dan Dan watersheds contain headwaters or riverine erosion zones that also feed marine protected areas, and in the Kagman watershed there are two shelter facilities below the erosion zone. In September of 2002, a large rain event caused mudslides and flooding in the Kagman, Capitol Hill, Achugao, San Rogue,Garapan, and other areas where erodible soils and urban flooding are frequent (NOAA NCEI, 2021). Erodibility factors above 0.02 are moderate to high probability and typically consist of Chinen sandy loams or gravels (USDA, 2021).

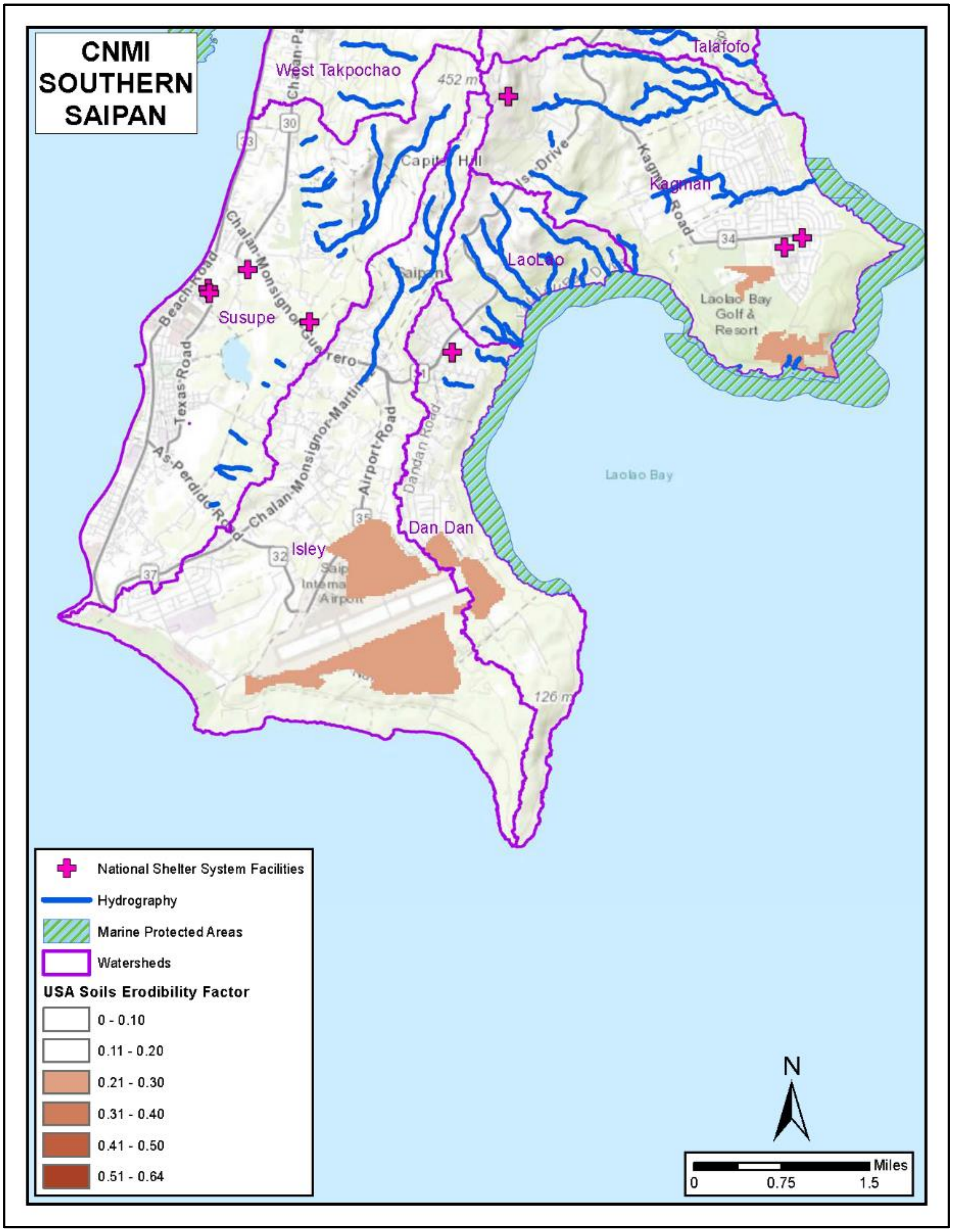

Figure 16. Southern Saipan Erodible Soil Watersheds and Impact Zones

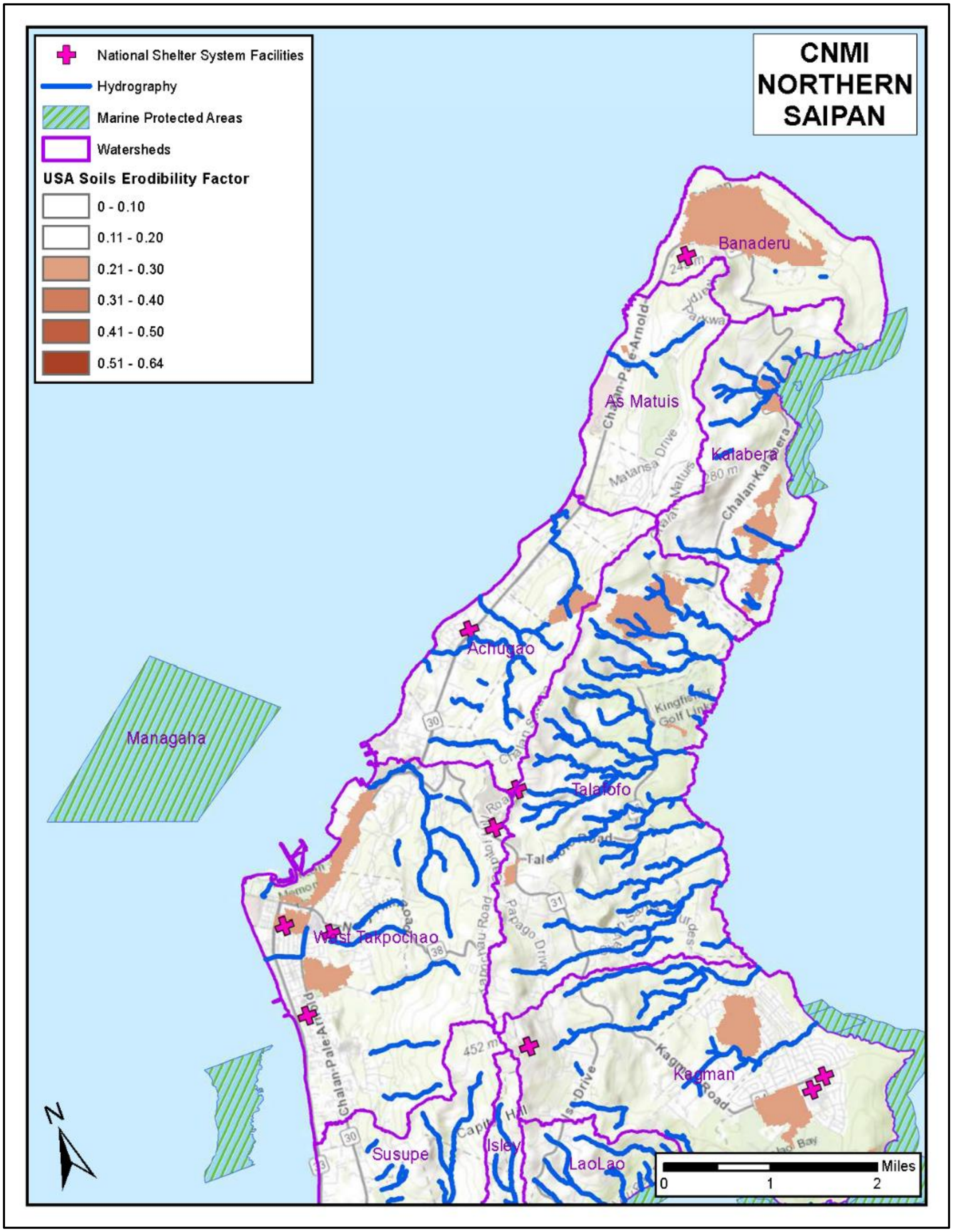

Figure 17. Northern Saipan Erodible Soil Watersheds and Impact Zones

The West Takpochao watershed, which drains to the west, conveys sediment toward Chalan Pale Arnold road, the American Memorial Park, Garapan Elementary School (a National Emergency Shelter), Beach Road, and nearshore waters and harbor, and the Lighthouse Reef Trochus Marine Sanctuary area. The Talofofo watershed headwaters, draining eastward, also contain erodible soils that can affect the development and near shore waters below it, including Route 31 and the headwaters to the north of Kingfisher Golf Links. In the Achugao watershed, which drains to the west, erodible soils can affect San Rogue and the Chalan Pale Arnold road below. The eastern draining watershed of Kalabera has two erosional zones with the northern most sub-basin draining into the Birds Island Marine Protected area. The far north watershed of Banaderu contains a significant area of erodible soils.

In addition to erodibility based on soil type and slope, the added vulnerability due to recent fire activity can accentuate erosion potential. The Achugao watershed experienced significant areal fire extent in 2016, 2017, 2018, and 2019. The Talofofo watershed experienced significant fire damage in 2016, 2017, and 2018. Figure 18 illustrates the central Saipan area watersheds with significant fire activity over the past five years.

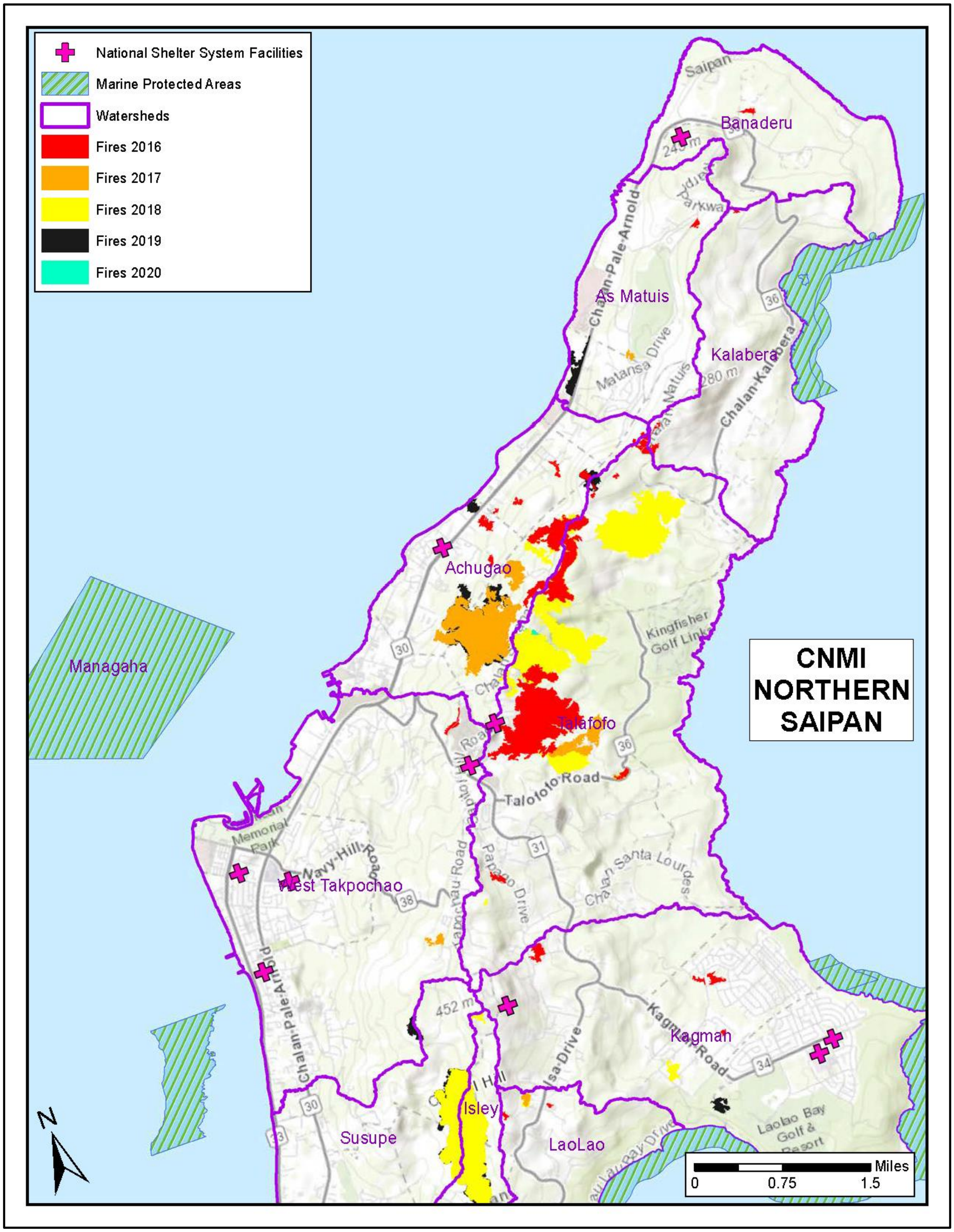

Figure 18. Significant Fire Zones in Saipan for Erosion

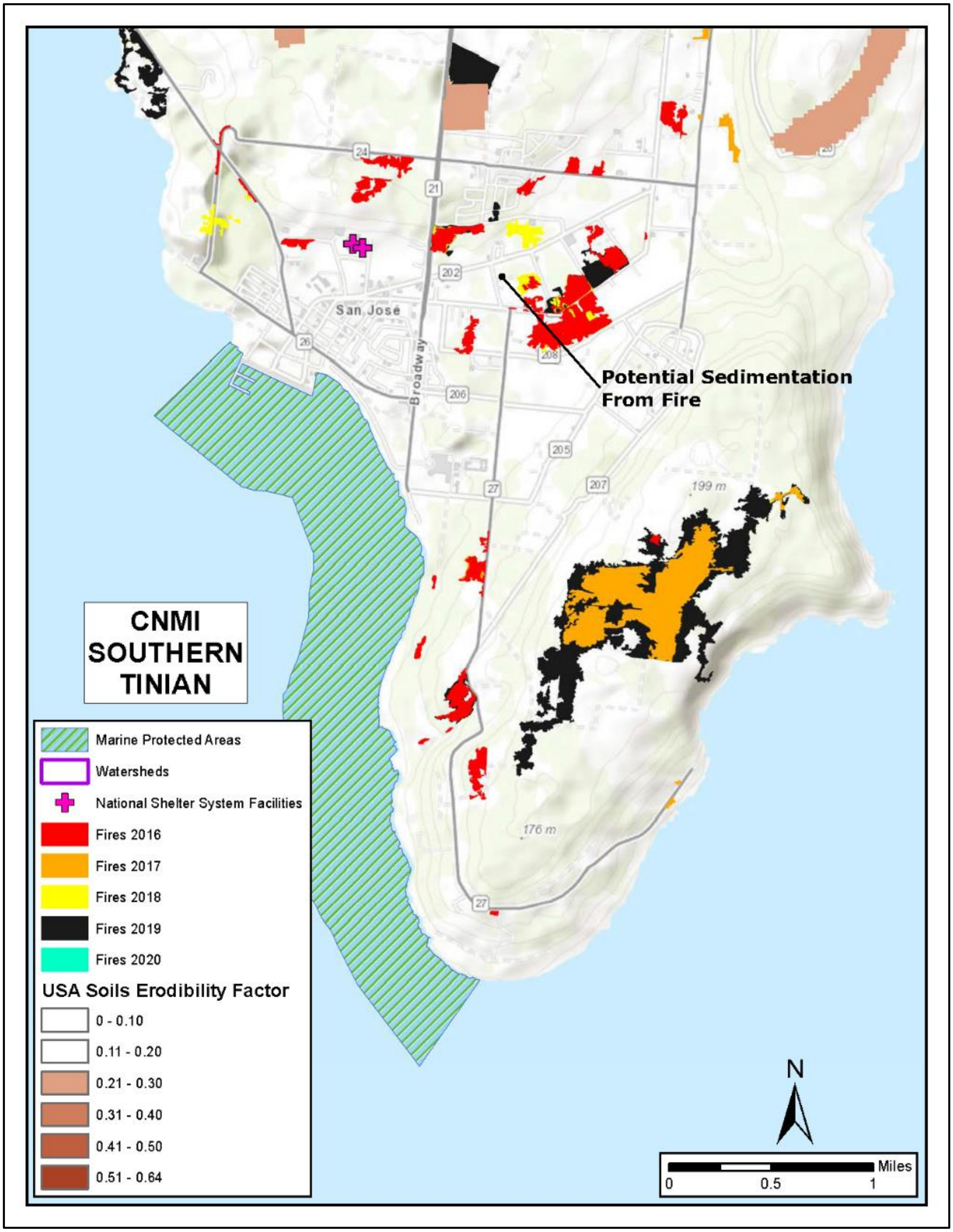
CNMI
SOUTHERN
TINIAN
Marine Protected Areas
Watersheds
National Shelter System Facilities
Fires 2016
Fires 2017
Fires 2018
Fires 2019
Fires 2020
USA Soils Erodibility Factor
0 - 0.10
0.11 - 0.20
0.21 - 0.30
0.31 - 0.40
0.41 - 0.50
0.51 - 0.64
Potential Sedimentation
From Fire
San José
Broadway
199 m
176 m
N
Miles
0
0.5
1

Figure 19. Southern Tinian Significant Fire Zones and Potential Erodibility

Tinian does not have surface streams, but sediment can be transported during heavy rainfall events into near shore waters and roadways. In southern Tinian, potential for erosion exists due to repeated fires east of San Jose. Figure 19 indicates where the valley between Route 208 and Route 202 are susceptible to sedimentation. Additionally, potential erosion from the large areal fire zone east of Route 207 is on a divide and drains to the east and west. Sediments conveyed to the west would impact the Tinian Marine Reserve protected area.

In northern Tinian, a highly erodible zone is observable adjacent to the airport (east of Route 21) and drains westward into a 2019 fire zone on the coast, north of San Jose. Figure 20 illustrates this area which contains both erodible soils and a fire damaged zone. The northeastern coastline of Tinian is highly fire damaged and a small fire damage zone rest above the highlighted wetland which is down slope of the 2018 fire.

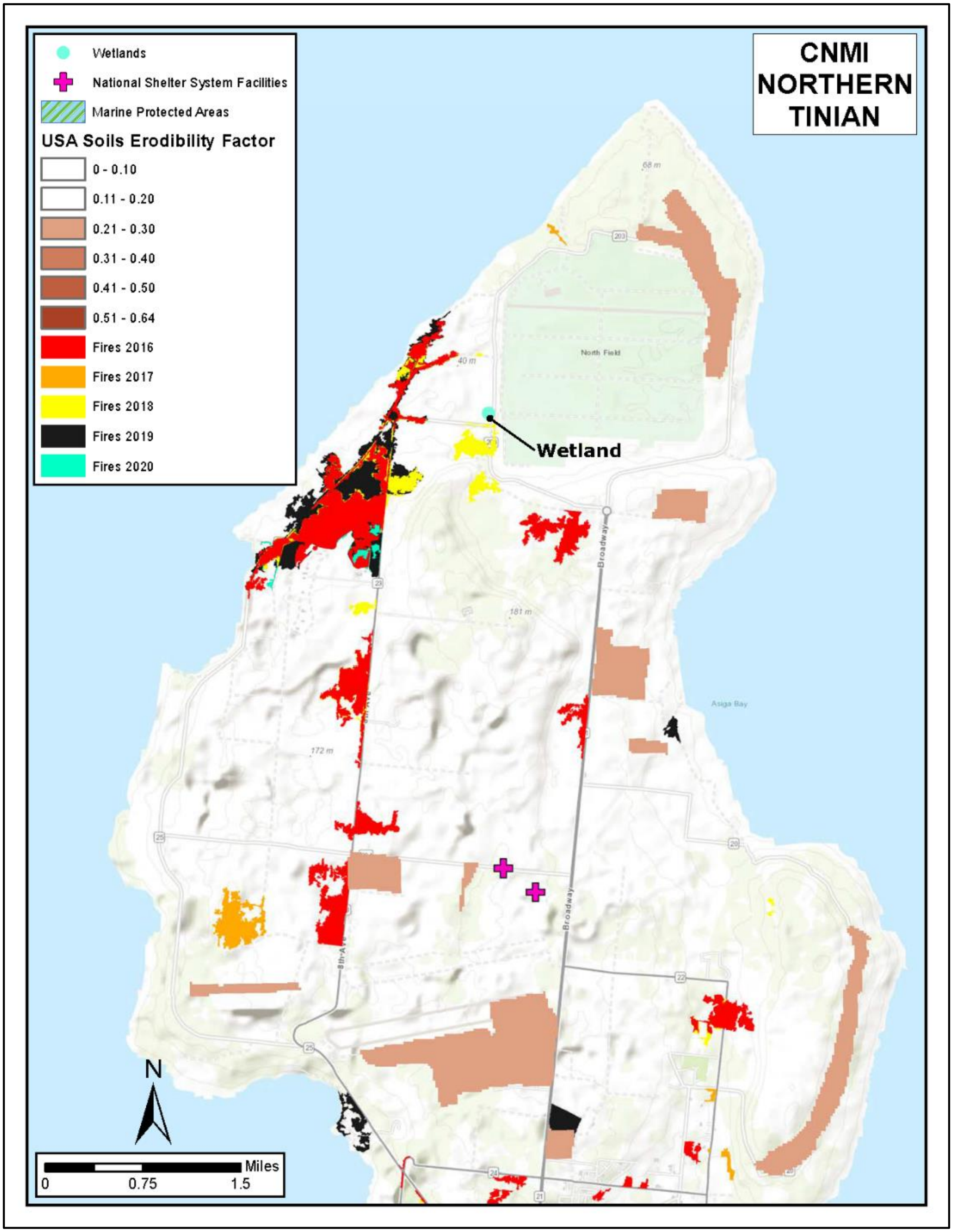
Wetlands
National Shelter System Facilities
Marine Protected Areas
USA Soils Erodibility Factor
0 - 0.10
0.11 - 0.20
0.21 - 0.30
0.31 - 0.40
0.41 - 0.50
0.51 - 0.64
Fires 2016
Fires 2017
Fires 2018
Fires 2019
Fires 2020
CNMI
NORTHERN
TINIAN
Wetland
North Field
Broadway
Asiga Bay
N
Miles
0
0.75
1.5

Figure 20. Northern Tinian Significant Fire Zones and Potential Erodibility

Graphical erosion and soil data were not available for Rota. Rota's parent soil material is coralline limestone which lies above an older volcanic basement. Volcanic rock outcrops are observable in southeast Rota and are the source of the limited clay soils on the island along the base of Mount Sabana. Rota soils are predominately Luta soil series and Takpochao Variant series with generally shallow depths, cobble, and loam texture, and erodible (USDA, 1989). The "badlands", in the southeast, contain acidic and highly erodible soils where forestation is difficult and soil chemistry leaches nutrient rich phosphorous from the soils. According to landslide hazard maps (Worldbank, 2020), The bluff near Mount Sabana, in Figure 21 , is a high hazard zone for rainfall activated landslides. Several residential buildings and the Sasanhaya Bay Fish Reserve (marine protected area) are downslope of the (Sabana Talakhaya Badlands) hazard zone. The Sabana Talakhaya region is presently under an Integrated Watershed Management Plan with the Office of Planning and Development for coral reef mitigation and water quality. Human induced fires are a major contributor to erosion, near shore sedimentation and water quality impacts.

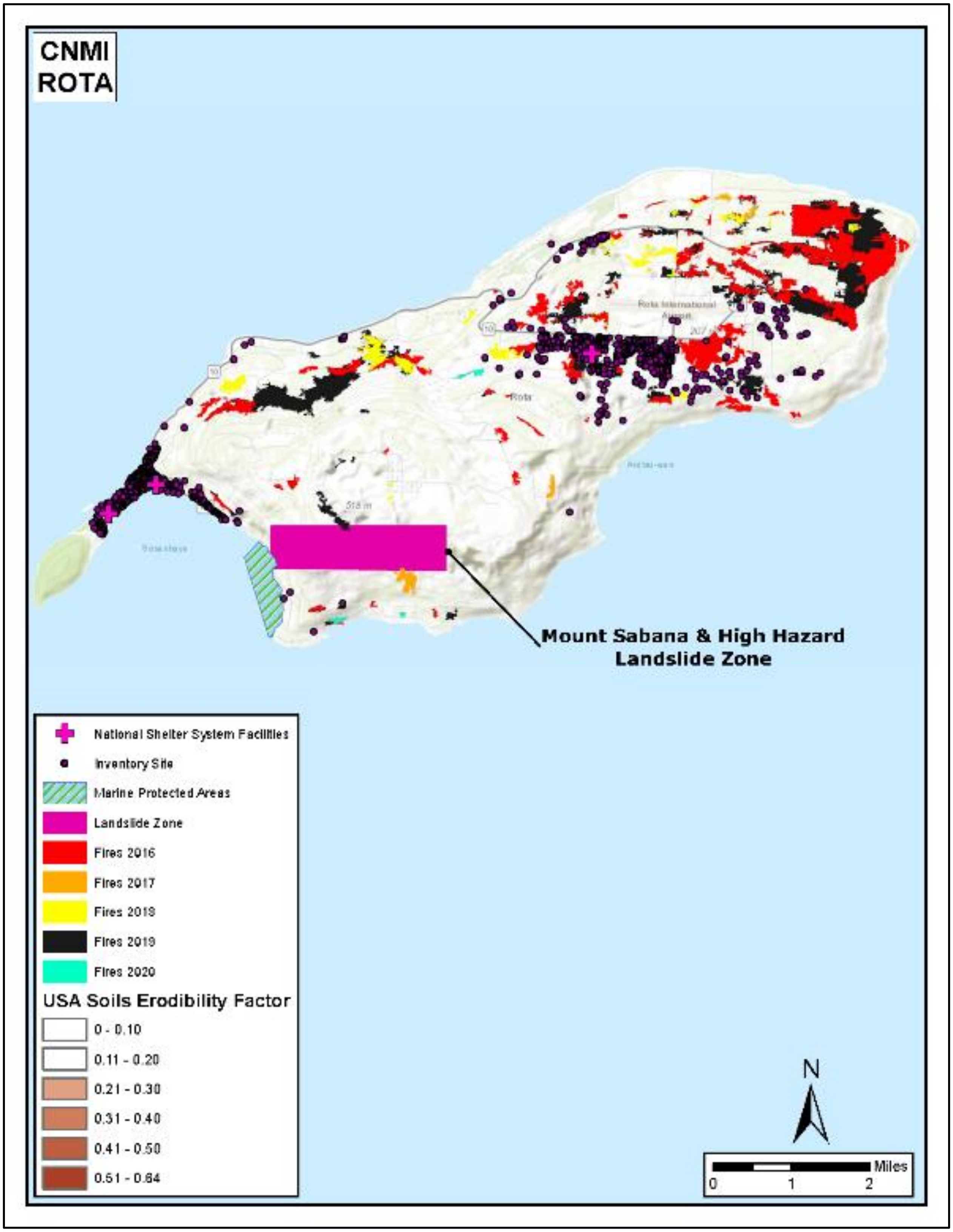
CNMI
ROTA
Mount Sabana & High Hazard Landslide Zone
National Shelter System Facilities
Inventory Site
Marine Protected Areas
Landslide Zone
Fires 2016
Fires 2017
Fires 2018
Fires 2019
Fires 2020
USA Soils Erodibility Factor
0 - 0.10
0.11 - 0.20
0.21 - 0.30
0.31 - 0.40
0.41 - 0.50
0.51 - 0.64
N
Miles
0
1
2

Figure 21. Rota Fire Damage - Erosion Potential and Landslide Locations

2.8 Seismicity

The Mariana Islands are part of a geologic structure known as the Izu–Bonin–Mariana Arc system, and range in age from 5 million years old in the north to 30 million years old in the south (Guam). The island chain arose because of the western edge of the Pacific Plate moving westward and plunging downward below the Mariana plate, a region which is the most volcanically active convergent plate boundary on Earth. This subduction region, just east of the island chain, forms the noted Mariana Trench, the deepest part of the Earth's oceans and lowest part of the surface of the Earth's crust. In this region, water trapped in the extensive faulting of the Pacific Plate, is heated by the higher temperatures of depth during its subduction, the pressure from the expanding steam results in the hydrothermal activity in the area and the volcanic activity which formed the Mariana Islands (Wikipedia- https://en.wikipedia.org/wiki/Mariana Islands).

Figure 22 illustrates the major subduction zones in the western Pacific region (NOAA[a], 2013). A USGS list of western Pacific earthquakes with magnitudes above 8.0 between 1900-2014 yields 14 historic earthquakes having a potential of triggering a local tsunami that would impact the vicinity of the Mariana Islands and are illustrated in Figure 23 (NOAA[a], 2013).

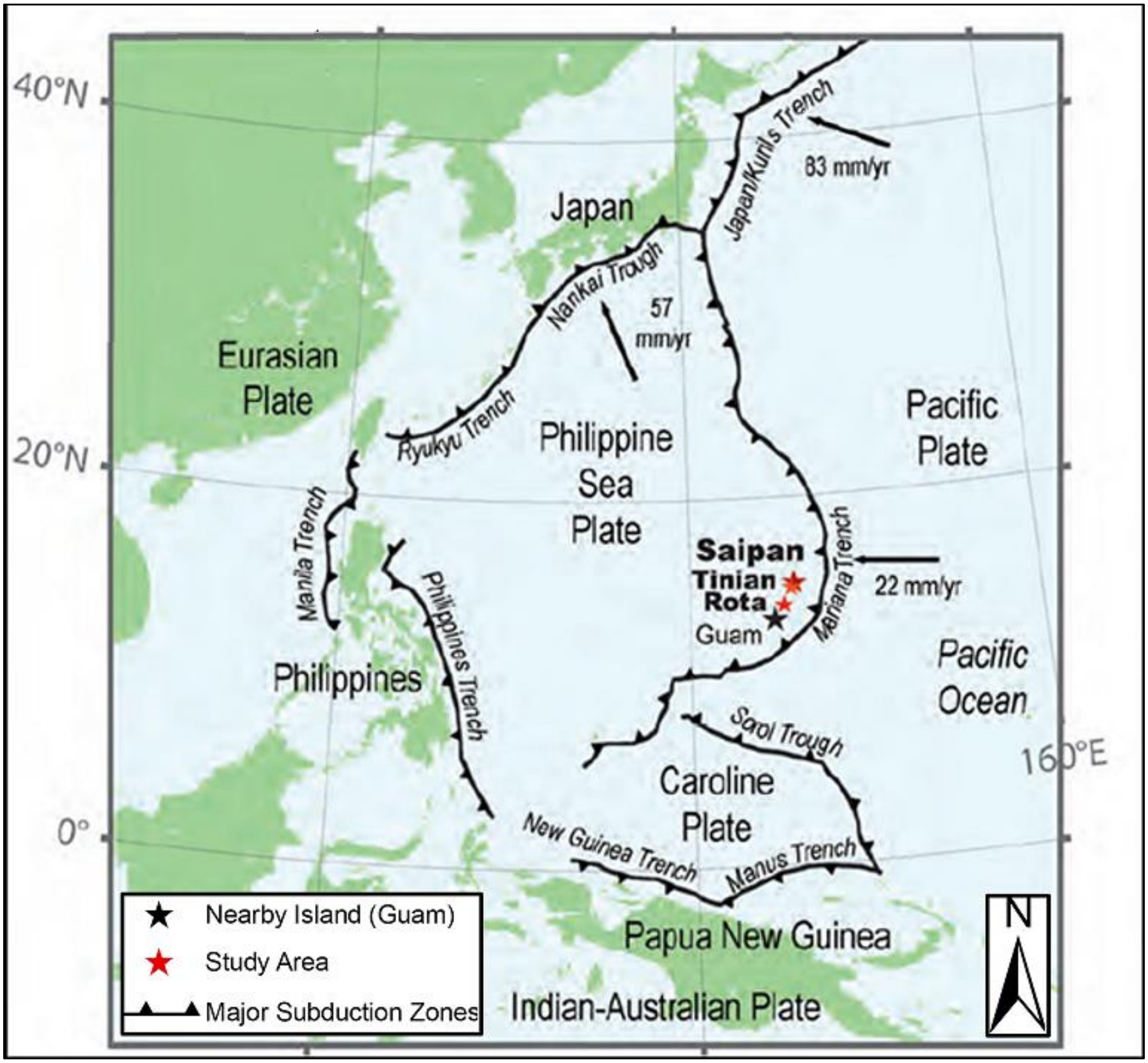

Figure 22. Regional Setting of CNMI Islands and Proximity to Major Subduction Zones

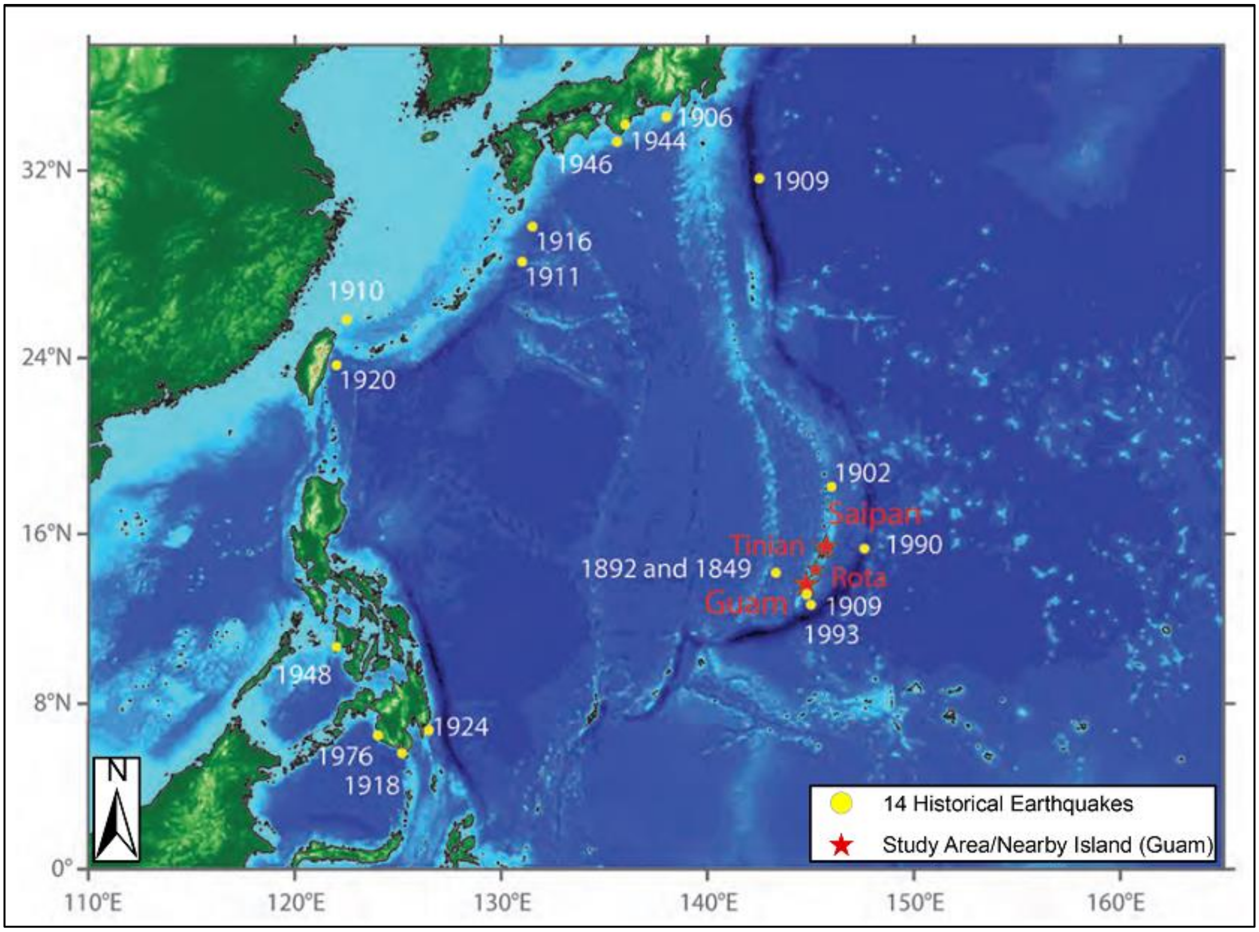

Figure 23. USGS Recorded Earthquakes > M 8.0 Since 1900

NOAA conducted a sensitivity study focused on the maximum computed wave amplitude and current speed to identify potentially hazardous tsunami sources (NOAA[a], 2013). A total of 349 M 9.0 synthetically generated tsunami source scenarios from around the Pacific Basin were modeled. A comparison of maximum amplitudes and currents predicted from each scenario with respect to the three individual islands suggests that each island is particularly sensitive to tsunamis generated from a specific direction. The maximum wave amplitude predicted for Saipan is 11.9 m (39.0 ft) for Onyan Beach along the southern side of Saipan from a synthetically generated event originating in the Mariana Trench. The maximum wave amplitude predicted for Tinian is 12.1 m (39.7 ft) for San Jose generated by a near-field event. The maximum wave amplitude predicted for Rota is 11.7 m (38.4 ft) in Sasanhaya Bay from the Kuril-Kamchatka-Japan subduction zone. The graphical results for Saipan, Tinian and Rota are shown in Figure 24, Figure 25 and Figure 26 respectively.

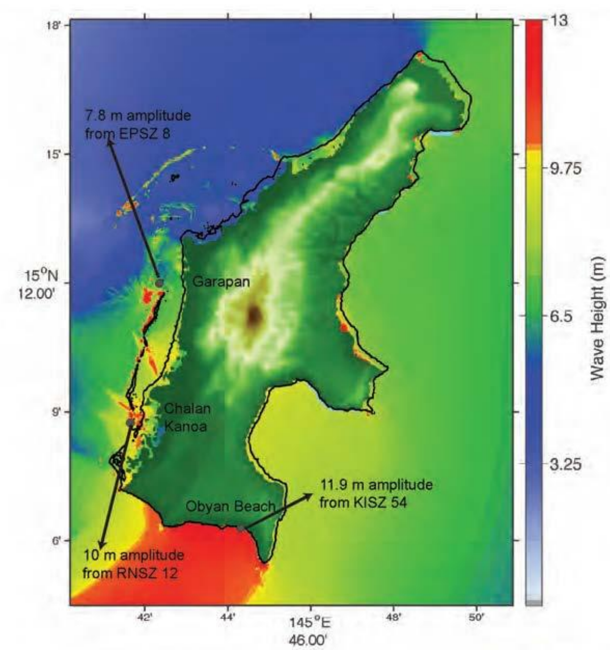

Figure 24. Saipan Maximum Tsunami Amplitudes

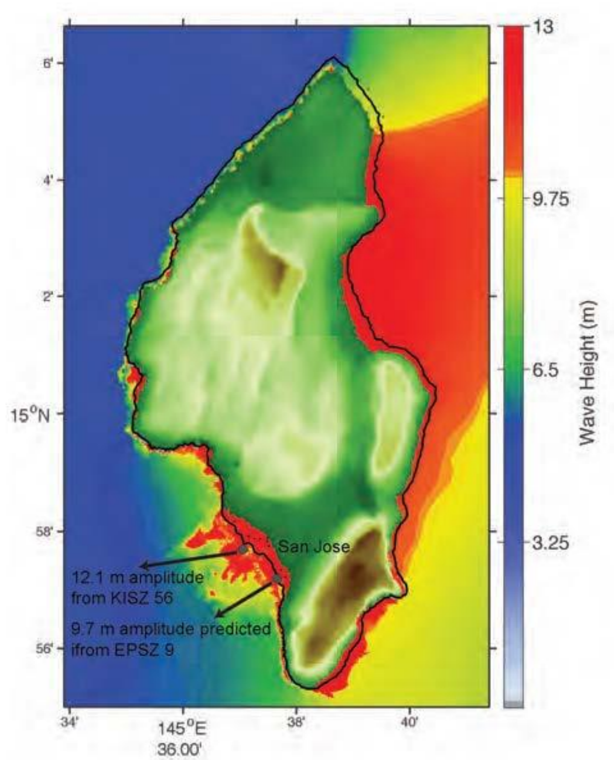

Figure 25. Tinian Maximum Tsunami Amplitudes

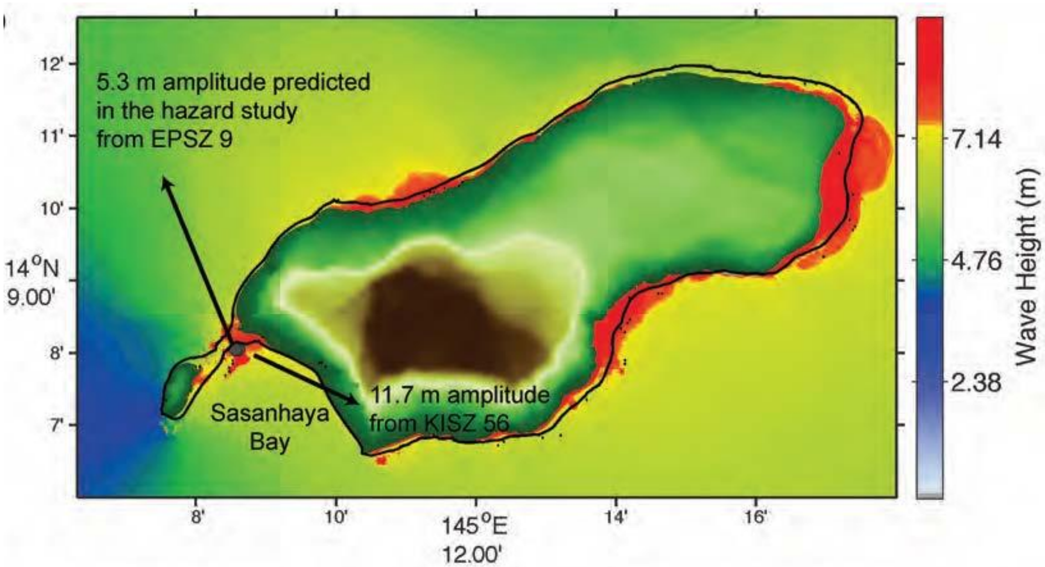

Figure 26. Rota Maximum Tsunami Amplitudes

2.9 Volcanism

The Mariana Volcanic Arc extends from 13°N to 23°N in the western Pacific Ocean, north of Guam. The Mariana region contains 9 volcanic islands and more than 60 submarine volcanoes, of which at least 20 are hydrothermally active. The summits of these submarine volcanoes range from 50 m to more than 1800 m below sea level. This one of the most active volcanic regions on Earth. The ocean crust that was formed along the mid-ocean ridges millions of years ago in the eastern Pacific is recycled back into the Earth's mantle as the ocean floor descends into the Mariana Trench. A portion of the ocean crust remelts and rises to the surface behind the trench along a line of submarine volcanoes and volcanic islands extending north of Guam for more than 1,000 kilometers. Many of the hydrothermally active sites we discovered are now part of the Mariana Trench Marine National Monument (Pacific Marine Environmental Laboratory) shown in Figure 27.

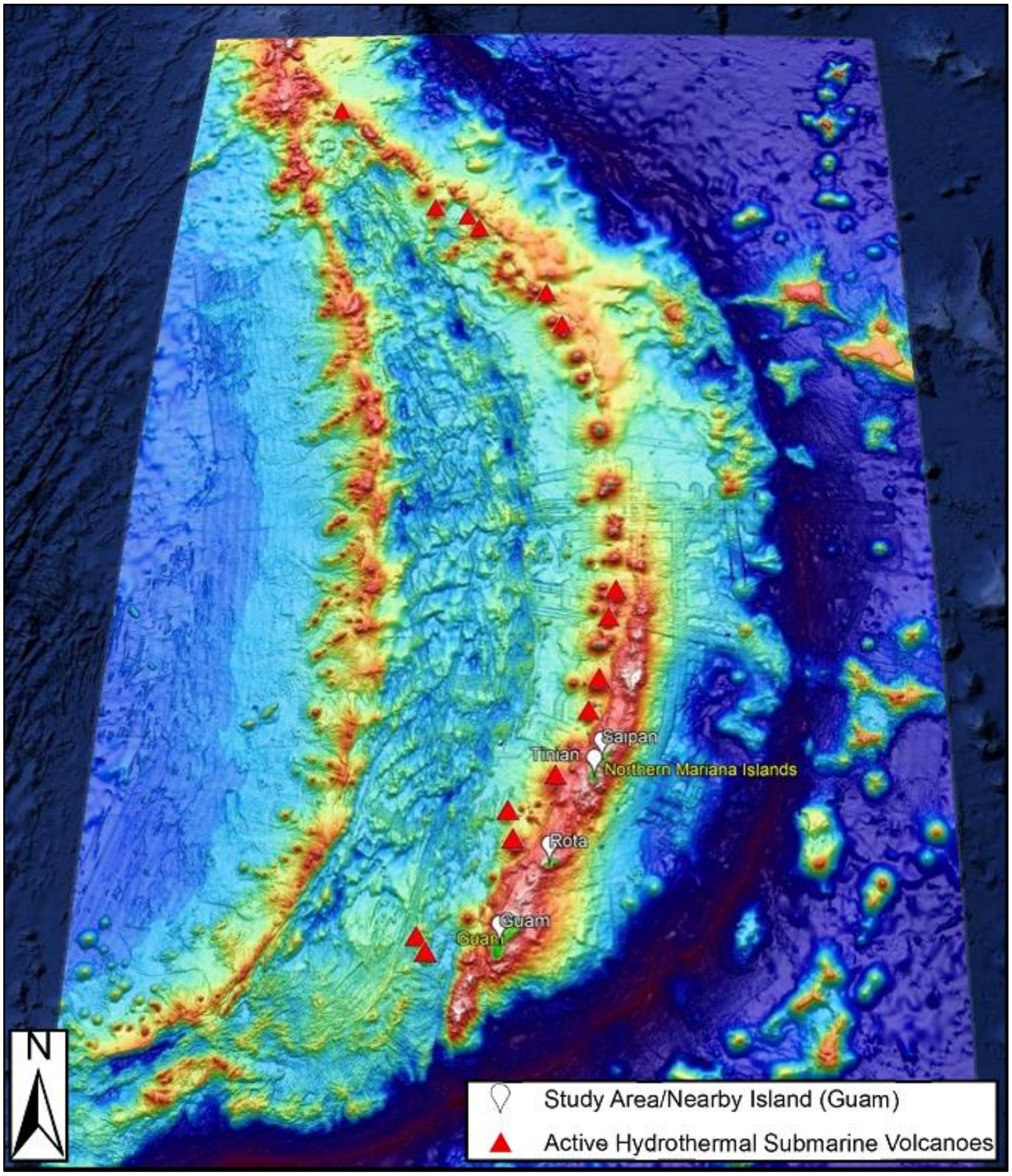

Figure 27. Mariana Volcanic Arc

2.10 Tsunamis

Many coastal communities and territories of the United States are at risk for tsunamis, and their infrequent occurrence gives communities a false sense of security. While tsunami hazards are infrequent, their consequences can be extremely high. Due to the relatively close distance to the tsunami generation locations, the population may have only minutes to hours to respond and reach a safe location. Tsunami sources include earthquakes, volcano's, sub-marine landslides, and seamount collapse, and meteorite strike. A tsunami generated close to the shoreline is termed a "near-field" tsunami, and a tsunami generated far from the source of impact is termed a "far-field" tsunami. Generally, it takes a magnitude >7.0 to generate a near-field damaging tsunami and >8.0 for a far-field tsunami (USGS[b], 2019). For example, a far-field earthquake centered in Chile would provide hours of notice while a near-field generated tsunami (Mariana Trench) may only provide minutes of notice. In some cases, a community may not feel an earthquake from a far-field earthquake or from a sub-marine landslide and therefore, be caught without warning. A local tsunami wave may arrive within minutes, emphasizing individuals need to understand natural cues such as ground shaking and shoreline draw down and immediately move to high ground. Alerts and warnings may not arrive in time.

After the 2004 Indian Ocean tsunami, which caused over 200,000 deaths, Congress passed two laws aimed to address potential tsunami damage: P.L. 1009-13 in 2005 (expanding tsunami detection networks) and P.L. 109-424 in 2006 (requesting NOAA and the National Tsunami Hazard Mitigation Program [NTHMP] to strengthen the nation's preparation, warning, and education efforts). NOAA receives annual funds for the NTHMP and each state/territory requests funds annually from the national program to administer their local programs. NOAA also sponsors the Tsunami Ready Community which is a voluntary program for states but does not require adherence to any methodology nor to administer enforcement.

The Pacific Tsunami Warning Center (TWC) in Honolulu, HI is the tsunami warning center serving the U.S. Pacific Territories. Tsunami alert systems and warning systems are categorically different. For example, a siren or audio alert alone does not provide information and direction. A TWC provides territory-wide information, direction, and updates. Sirens are locally effective as to the imminent hazard and may not be heard by individuals if indoors, outside of an audible radius, or during heavy rainfall. Siren require maintenance and can be difficult to replace in remote locations. Radio, social media, texts, and NOAA weather radio will provide more warning information than an alarm.

Six credible tsunamis were observed in the Mariana Islands since 1837 occurring in 1837, 1849, 1892, 1990, 1993 and 2011. The 1849 tsunami is believed to be the only one to have caused a fatality in the region.

The 2011 Tohoku earthquake (Japan/Kuril Trench) tsunami flooded Saipan, triggering surges in Apra Harbor and damaged a U.S. Navy vessel in port. The Apra Harbor (Guam) gage recorded a 4.3-foot increase in still water elevation, and the Pago Bay tide gage recorded a 1.6-foot surge within 3.5 hours of the earthquake. (NOAA OAR, 2010). The 1993 tsunami occurred during Typhoon Steve. Multiple hazards can occur simultaneously, and it is possible a sheltering center safe from coastal or riverine flooding may not be in a safe zone for tsunamis.

Modeling of high-resolution case and synthetic runs utilizing 349 potential 9.0 M earthquake scenarios (near and far field sourced earthquakes) were performed using the NOAA Method of Splitting Tsunami (MOST) model. Comparing maximum amplitudes and currents predicted from each scenario with respect to Saipan, Tinian, and Rota suggest each island is particularly sensitive to the specific direction of the generated tsunami. Table 4 lists the 26 scenarios posing the most significant risks to CNMI's vulnerable locations. Wave amplitudes are meters above Mean Higher High Water (MHHW).

Table 4. Predicted Tsunami Amplitudes for Worst Case Scenarios

	Saipan		Tinian		Rota	
Subduction Zone	Amplitude (m)	Current (m/s)	Amplitude (m)	Current (m/s)	Amplitude (m)	Current (m/s)
Aleutians–Cascadia	2.8	5.3	1.2	2.4	0.7	1.6
Aleutians–Cascadia	3.0	5.4	1.3	2.4	0.7	1.7
Aleutians–Cascadia	2.6	5.4	1.0	2.5	0.7	1.8
Aleutians–Cascadia	2.3	5.2	1.2	2.4	0.7	1.8
Aleutians–Cascadia	2.4	5.5	1.0	2.5	0.6	1.4
Aleutians–Cascadia	0.6	1.5	0.4	0.7	0.2	0.4
Aleutians–Cascadia	0.7	2.1	0.5	1.6	0.3	0.5
Aleutians–Cascadia	0.7	2.1	0.5	1.7	0.3	0.3
East Philippines	7.8	10.7	3.2	6.5	1.3	2.0
East Philippines	7.7	10.4	9.7	13.8	5.3	6.7
Kuril-Kamchatka–Japan	4.4	6.3	1.9	4.2	0.7	1.3
Kuril-Kamchatka–Japan	3.6	5.3	1.6	2.5	0.6	1.4
Kuril-Kamchatka–Japan	11.9	13.5	9.8	10.3	4.8	7.4
Kuril-Kamchatka–Japan	11.9	19.3	11.9	16.3	9.0	10.3
Kuril-Kamchatka–Japan	9.3	10.4	10.6	15.8	10.8	13.9
Kuril-Kamchatka–Japan	9.5	11.0	12.1	17.3	11.7	13.1
Manus OCB	3.2	5.2	1.4	2.4	0.6	1.1
Manus OCB	4.0	6.0	1.3	2.4	0.7	1.4
New Guinea	1.9	3.9	4.0	2.4	0.8	1.5
New Guinea	2.6	4.3	1.6	3.2	0.7	2.4
New Guinea	2.4	4.5	2.4	3.3	0.7	2.4
Ryukyu–Nankai	5.5	6.7	4.2	8.3	3.0	4.5
Ryukyu–Nankai	4.6	5.6	3.4	6.9	2.9	4.9
Ryukyu–Nankai	10.0	9.6	4.9	8.8	2.1	2.5
Ryukyu–Nankai	9.8	13.9	4.3	8.9	2.0	2.2
Ryukyu–Nankai	7.8	10.7	3.2	6.5	1.3	2.0

Figure 28 and Figure 29 illustrate the Probable Maximum Tsunami (PMT) wave run up under the worst-case conditions described in Table 3, as well as National Emergency Shelter locations impacted in tsunami hazard zones. Inundation files for Rota and Saipan were not available.

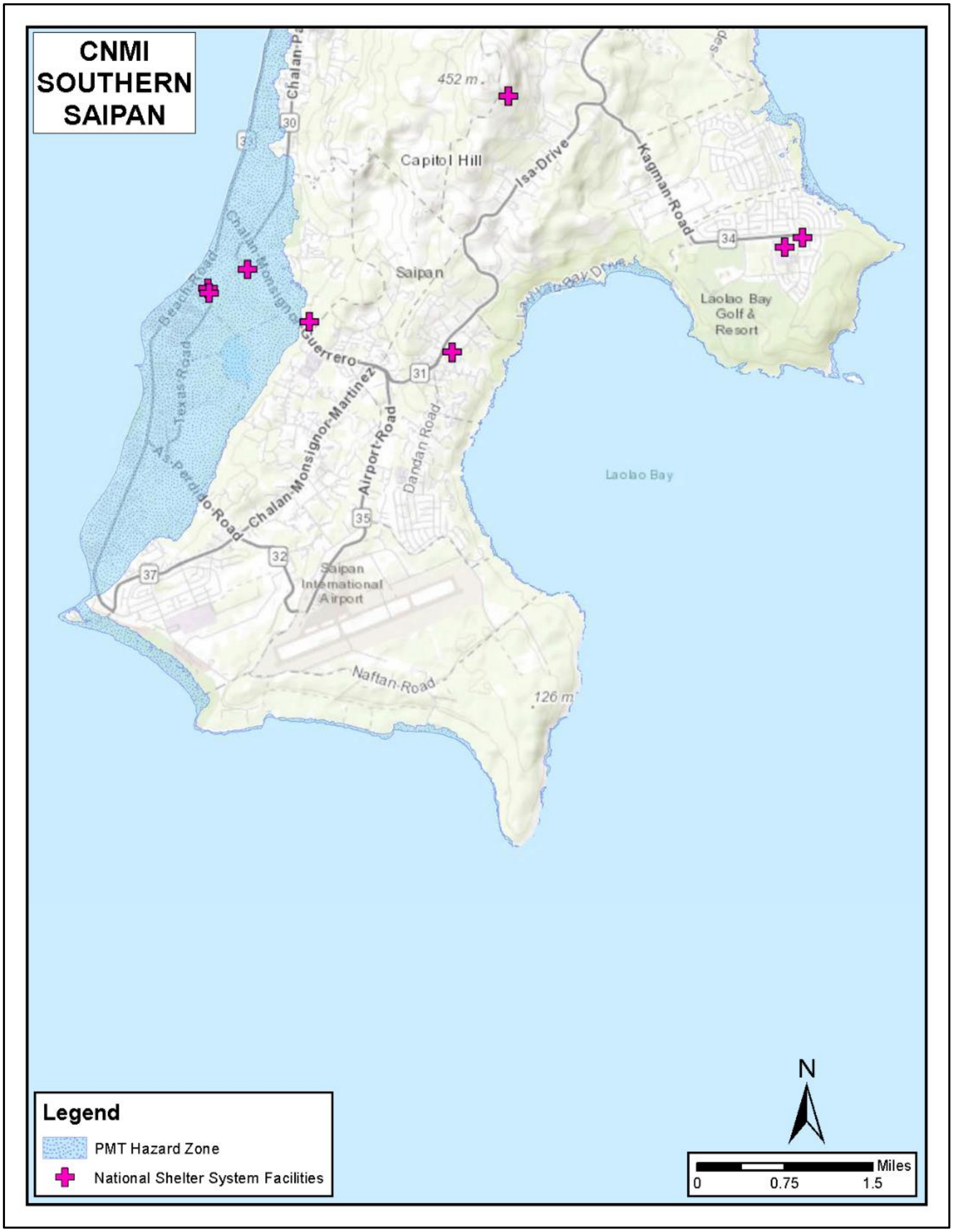

Figure 28. Southern Saipan, PMT Hazard Zone and National Shelter Locations (NOAA OAR, ESRI)

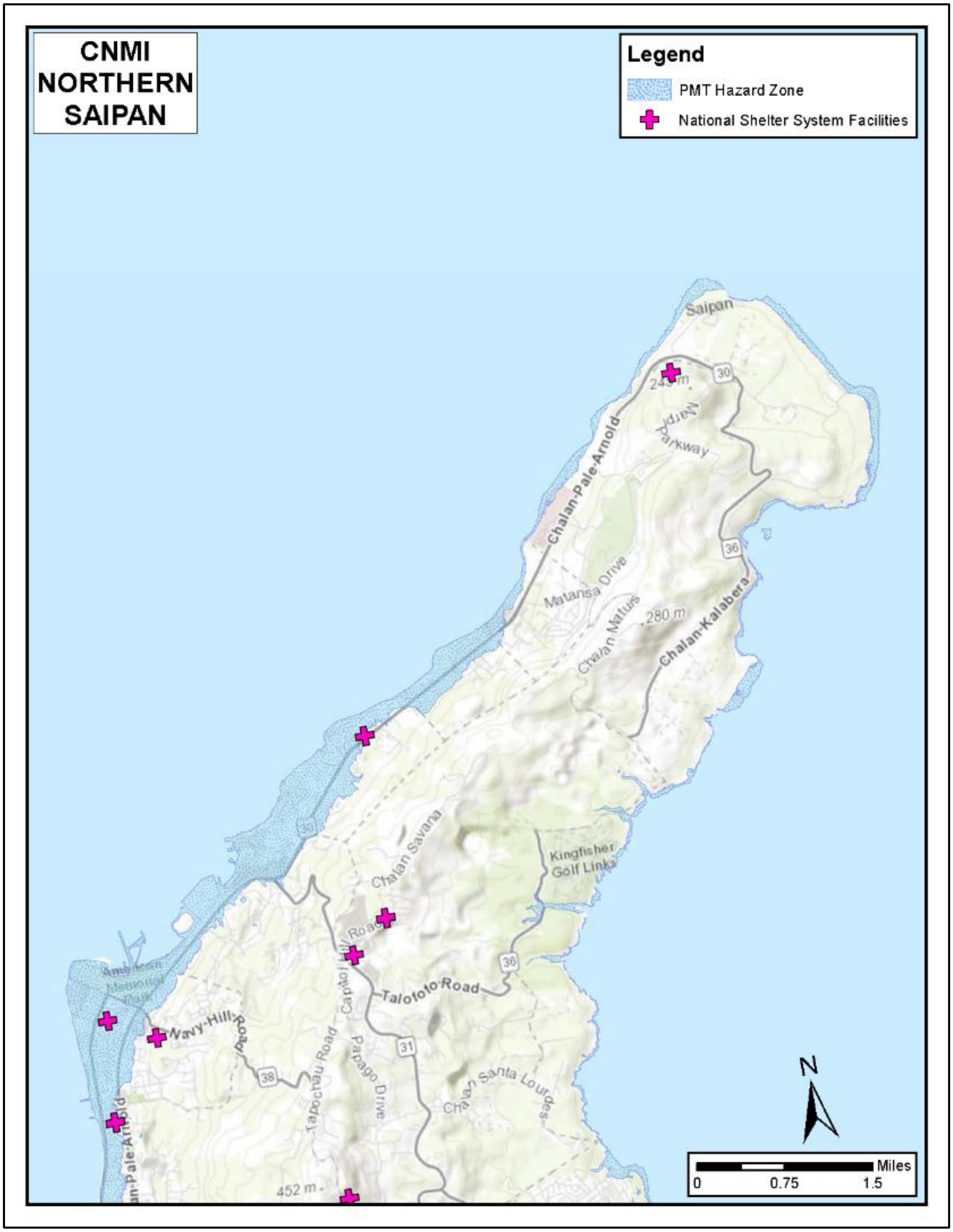

Figure 29. Northern Saipan, PMT Hazard Zone and National Shelter Locations (NOAA OAR, ESRI)

3. Vulnerability and Exposure: Future Conditions

USACE projects, programs, missions, and operations have generally proven to be robust enough to accommodate the range of natural climate variability over their operating life spans. However, recent scientific evidence shows that in some places and for some impacts relevant to USACE operations, climate change is shifting the climatological baseline about which that natural climate variability occurs and may be changing the range of that variability as well. This is relevant to USACE because the assumptions of stationary climatic baselines and a fixed range of natural variability as captured in the historic hydrologic record may no longer be appropriate for long-term projections of the climatologic parameters, which are important in hydrologic assessments for inland watersheds (USACE, 2020).

To evaluate the impacts of climate change on the study area's hydrometeorology a qualitative climate assessment is carried out in accordance with ECB 2018-14, Guidance for Incorporating Climate Change Impacts to Inland Hydrology in Civil Works Studies, Designs, and Projects. As indicated by the flow chart in Figure 30, the qualitive assessment includes a literature review examining trends in historic, observed, and projected, future temperature, precipitation, and streamflow. The literature review is conducted at both the western Pacific (regional) and Island (local) scale. The assessment requires a quantitative evaluation of trends and nonstationarities in observed hydrometeorological records relevant to the study area and purpose. The final component of the ECB 2018-14 analysis is a review of projected climate changed hydrology and a screening level vulnerability assessment specific to the USACE business lines associated with the study objective.

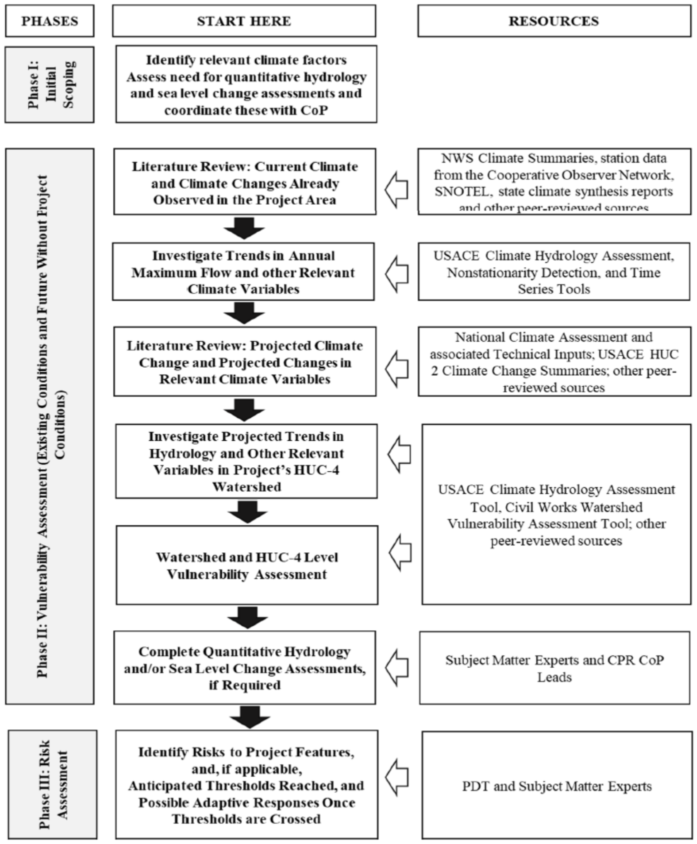

Figure 30. Flow chart describing steps for a qualitative assessment of impacts of climate change in hydrologic analysis (ECB 2018-14)

3.1 Literature Review

To summarize trends in observed and projected temperature, precipitation, and streamflow the Climate Science Special Report from the Fourth National Climate Assessment (NCA4) (USGCRP, 2018) and the USACE's synthesis of Recent US Climate Change and Hydrology Literature Applicable to US Army Corps of Engineers- Hawaii Region (USACE (2015)) are referenced but do not explicitly describe CNMI. Sources used in developing this report are from the 2021 report labeled "2021: Climate Change in the Commonwealth of the Northern Mariana Islands: Indicators and Considerations for Key Sectors" by Grezni, Z. et all.In this document projections of streamflow, temperature and precipitation are predominantly presented using this data.

3.2 Assessment of Climate Change Impacts to Inland Hydrology

The focus of the inland hydrology assessment is the flood risk management business line and the high flow regime. Large-scale floods can instigate streambank erosion and are critical to any future project performance. Consequently, the focus of the first order statistical analysis conducted as part of this assessment is on peak flow. Observed data is analyzed using the annual instantaneous peak flow records on the Island. Projected, future streamflow data cannot be visualized using the Vulnerability Assessment Tool as these products have only been developed for Hydrologic Unit Codes (HUC)'s within the Continental US.

3.3 First Order Statistical Analysis – Observed Streamflow Gages Analyzed

ECB 2018-14 requires a first order statistical analysis of timeseries relevant to the study purpose. First order statistical analysis encompasses a range of easily applied statistical tests including trend analysis and nonstationary analysis. The focus of first order statistical analysis is trend and nonstationary in annual instantaneous peak streamflow data, observed at the USGS stream Gage on the Island of Saipan, CNMI HUC 22020000. In general, annual peak streamflow is appropriate for this analysis because infrequent, large-scale floods can instigate streambank erosion. USGS Gage 1680100, SF Talufofo Stream at Saipan CNMI Gage 1680100 listed in Table 5 has a 24-year period of record from 1968 through to 1994 and will be presented.

Table 5. USGS Stream Gage at CNMI

Site Number	Station Name	Drainage Area (sqm)	Period of Record	30 Years of Continuous Record?
16801000	SF Talufofo Stream, Saipan, CNMI	0.69	1968 - 1994	No

3.4 Nonstationary & Trend Analysis

ETL 1100-2-3, Guidance for Detection of nonstationarities in Annual Maximum Discharges is applied to evaluate the assumption of stationarity in the study area. The USACE Nonstationary Detection (NSD) Tool were applied to assess whether the annual instantaneous peak streamflow records collected at the Gage locations listed above are representative of stationary hydrologic conditions. For trend analysis, a p-value threshold of 0.05 is adopted to be indicative of statistical significance. Results described in this document have been created using the tools available in the Time Series Toolbox (TST) located at https://climate-test.sec.usace.army.mil/tst_app/. Analysis of the 24-year period of discharge data from the USGS Gage 1680100, South Fork Talufofo Stream at Saipan CNMI was loaded and analyzed using the Time Series toolbox and the results are shown below in Figure 31and Figure 32 below.

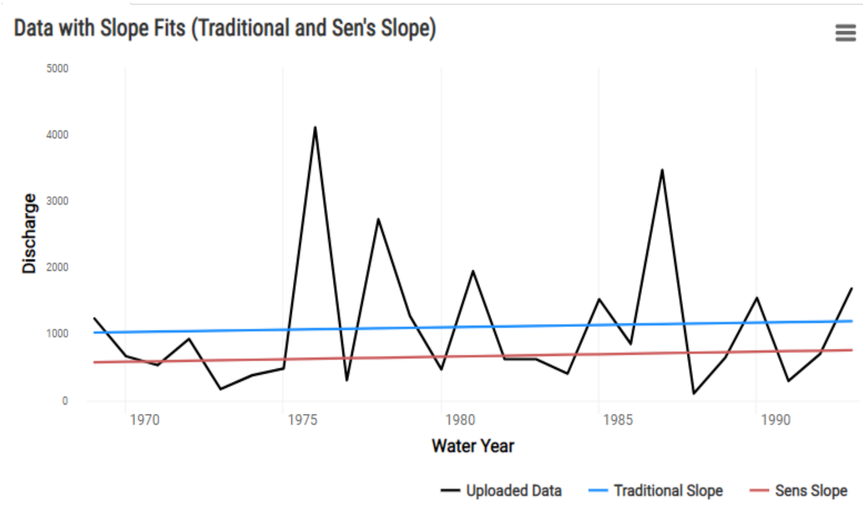

Trend Line Coefficients

Method	Slope	Intercept
Traditional Slope	7.0877	-12936
Sen's Slope	7.6	-14392

Figure 31. Time Series Toolbox- Annual Peak Discharges

Test	P.Value
t-Test	0.80837
Mann-Kendall	0.67412
Spearman Rank-Order	0.63299

- **A statistically significant trend (at the alpha = .05 level) was NOT detected by the Mann-Kendall Test.**
- **A statistically significant trend (at the alpha = .05 level) was NOT detected by the Spearman Rank-Order Test.**

Source: 16801000.csv

Figure 32. Time Series Toolbox - Annual Peak Discharge P-Value

For a nonstationarity to be considered strong it must demonstrate a degree of consensus and robustness. To show consensus the nonstationarity must trigger two or more tests within a range of five years for the same statistic (distribution, mean, etc.). To demonstrate robustness, it must trigger two or more tests within a range of five years for different statistics. A strong nonstationarity must also show significant change in the magnitude of the standard deviation and/or mean (USACE, 2017). Although this dataset does not have 30 years of continuous record the summary results of the nonstationarity test and the Trends Analysis are described in

Table 6.

Table 6. Monstationarity Test & Trends Result

Site Number	Station Name	Nonstationary Test & Trends Results
16801000	SF Talufofo Stream, Saipan, CNMI	-Analysis for the 1968 – 1994 period- - No nonstationarities detected. - No statistically significant trends were detected - Analysis shows a mildly positive trend.

Nonstationary analysis of peak streamflow can detect changes, gradual or abrupt, in hydrologic processes over the period of record and an analysis was conducted for the Gage listed in above. Streamflow records for CNMI are virtually non-existent as the only stream Gage available is the USGS Gage 1680100, SF Talufofo Stream at Saipan CNMI. Gage has 1680100 has a 24-year period of record from 1968 through to 1994. As this period of record falls short of the desired 30 years of record, a correlation analysis was conducted using USGS stream Gages at Guam to evaluate their effectiveness for use as a proxy for climate change. The four Gages used for this evaluation are listed in Table 7 below.

Table 7. USGS Stream Guages - Guam

Site Number	Station Name	Drainage Area (sqm)	Period of Record	30 Years of Continuous Record?	Correlation Coefficient
16801000	SF Talufofo Stream, Saipan, CNMI	0.69	1968 - 1994	No	
16847000	Imong River near Agat, Guam	1.92	1961 - 1993 1998 - 1999 2001 - 2004 2006 - 2019	No	0.41
16848100	Almagosa River near Agat, Guam	1.32	1972 - 1991 1998 - 2019	No	0.45
16848500	Maulap River near Agat, Guam	1.18	1972 - 1993 1998 - 2015 2017 - 2020	No	0.43

The results of the correlation between the stations in Guam and CNMI enumerated in Table 7 show only a moderate correlation strength and a positive correlation type. As we prefer to have a very strong positive correlation type (correlation strength greater than 0.7) when evaluating drainage areas for use as a proxy we found they could not be used.

Precipitation data can also be a good indication of nonstationarity. Precipitation records in the CNMI contain significant gaps and are not representative of the geography of the islands. Thus, CNMI rainfall data is deemed inadequate for climate studies. The nearest station with sufficient data, and thus considered the best available record relevant to the CNMI, is at Andersen Air Force Base in Guam. Using annual precipitation data collected from 1991 – 2020 show that there are no nonstationarities detected, no statistically significant trends showing a mildly rising trend.

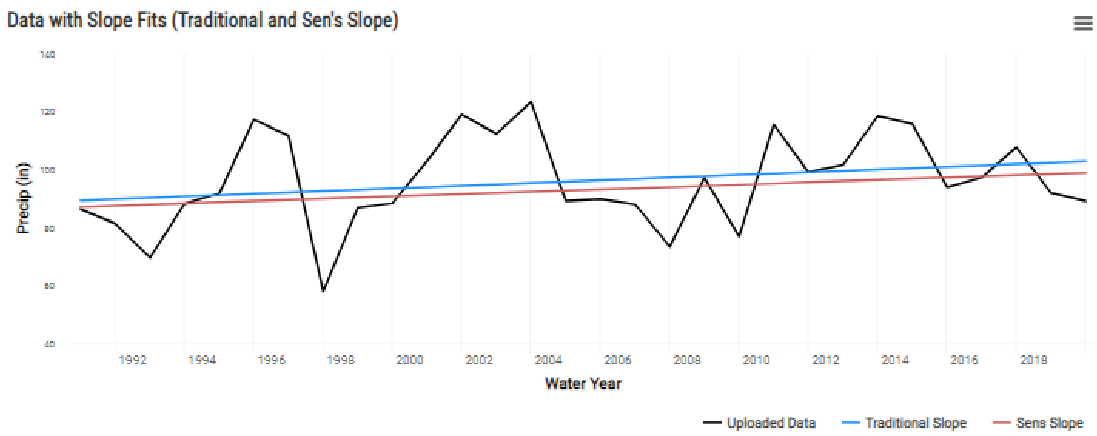

Trend Line Coefficients

Method	Slope	Intercept
Traditional Slope	0.46432	-835.17
Sen's Slope	0.40529	-719.87

Source: Guam_Annual_Precip1.csv

Figure 33. Time Series Toolbox - Annual Precipitation Trends

Visualization | Trend Hypothesis Test

Test	P.Value
t-Test	0.17568
Mann-Kendall	0.10072
Spearman Rank-Order	0.080117

- **A statistically significant trend (at the alpha = .05 level) was NOT detected by the Mann-Kendall Test.**
- **A statistically significant trend (at the alpha = .05 level) was NOT detected by the Spearman Rank-Order Test.**

Source: Guam_Annual_Precip1.csv

Figure 34. Time Series Toolbox - Annual Precipitation P-Values

3.5 Air Temperature

Reference (Grezni, Z., 2021). The longest complete air temperature dataset for the Mariana Islands available from NOAA is the Anderson Air Force Base (Guam) record from 1953 to 2002. Recent data (after 2002) are not available from NOAA for this station. Although temperature records for Saipan, Tinian, and Rota do exist, they are mostly short and discontinuous. A continuous record of 30 years is more generally considered suitable for climate studies.

The annual number of hot days in the Mariana Islands has increased (see Figure 35 and Figure 36). Days with temperatures at or above 88°F recorded at the Anderson Air Force Base weather station have increased, on average 5 days per year exceeding 88°F in the 1950’s, compared to

36 days per year on average in the 1990's. Recent air temperature measurement at the Francisco C. Ada Saipan International Airport also shows an increasing trend in the annual number of hot days 90°F or warmer since 2006.

Note: Figure 35 represents the annual number of days with temperature 88°F or hotter (at of above the 95th percentile of the data record) at the Anderson Air Force Base in Guam from 1953 to 2002. The trendline (black, dotted line) shows there has been a long-term increase in the annual number of hot days. Figure 36 represents the annual number of days with maximum temperatures at or above 90°F- the 95th percentile of the data record recorded at the Francisco C Ada Saipan International Airport from 2006 to 2020. Original figures by Abby Frazier using data from the NOAA GHCN-Daily database for 1953-2002. (Grecni, Z., 2021)

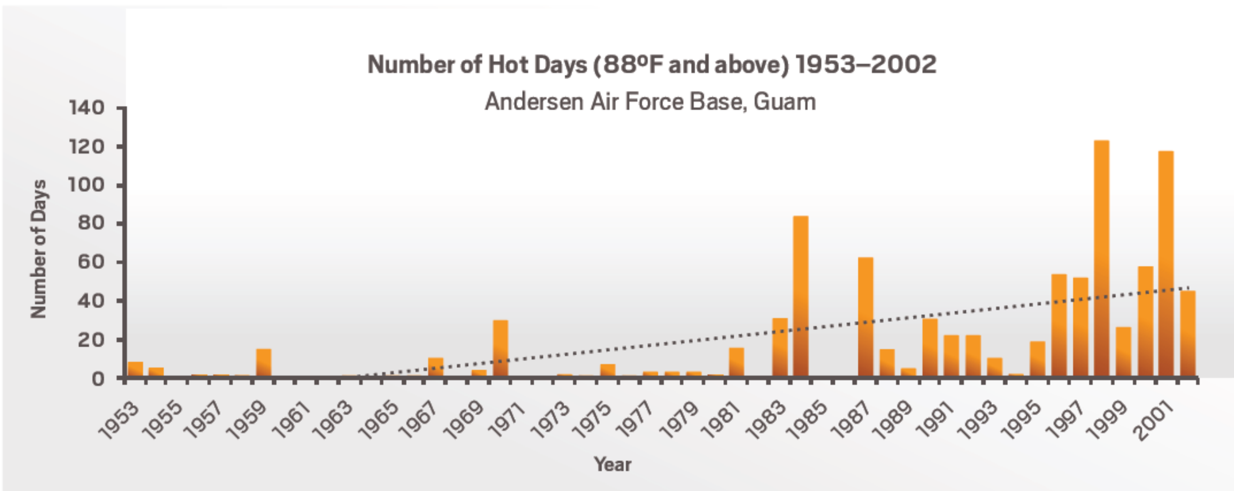

Figure 35. Annual number of days with maximum temperature at or above 88°F

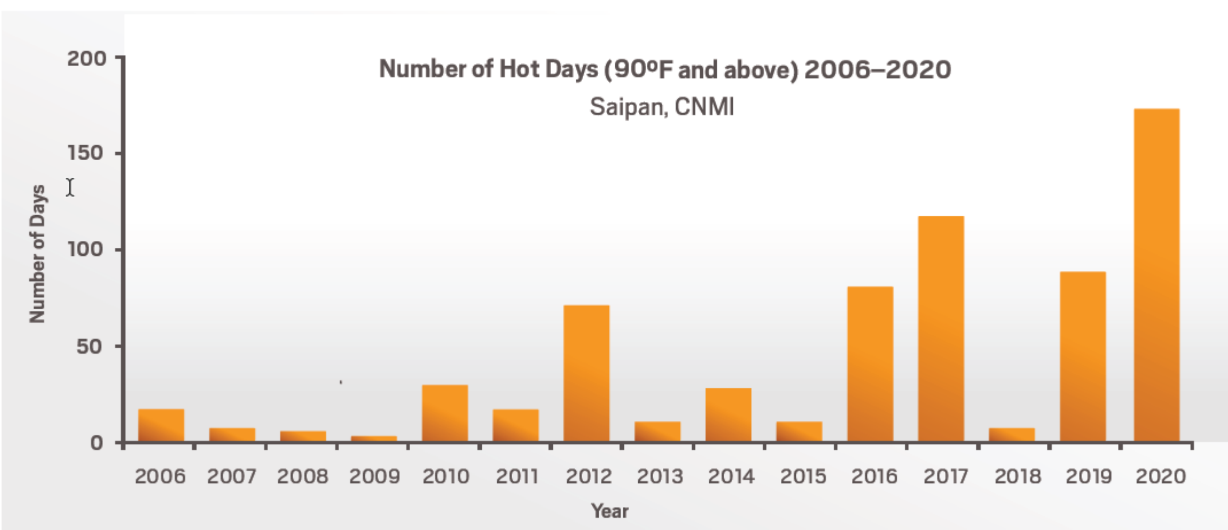

Figure 36. Annual number of days with maximum temperature at or above 90°F

Similarly, there has been a drop in the annual number of cool nights (below 74°F, or 23.3°C) observed at Andersen Air Force Base between 1953 and 2002 and at the international airport in Saipan from 2006 to 2020 (Figure 37 and Figure 38; NOAA, 2020).

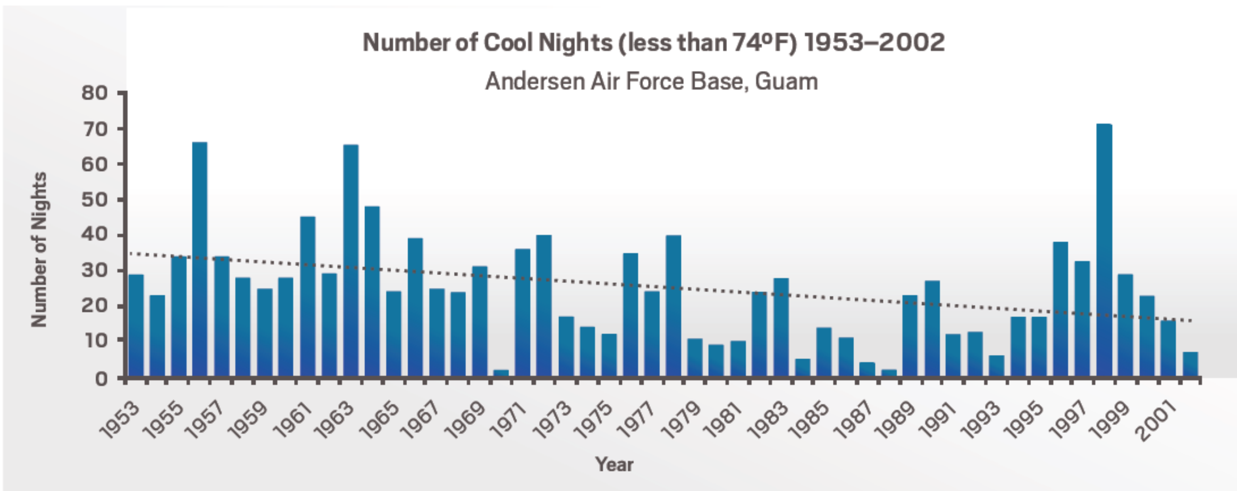

Figure 37. Number of Cool Nights Less than 74°F (1953-2002)

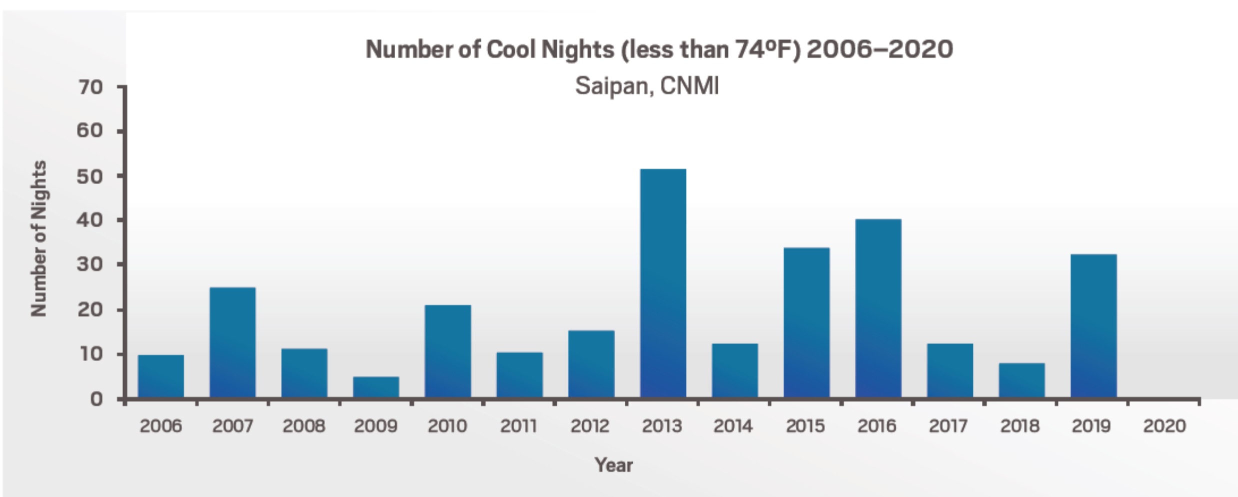

Figure 38. Number of Cool Nights Less than 74°F (2006-2020)

Note: Figure 37 represents the Annual number of nights with minimum temperature less than 74°F, the10th percentile of the data record, at Andersen Air Force Base in Guam from 1953 to 2002. The trendline (black, dotted line) shows a decrease on average in the frequency of cool nights during 1953–2002.Figure 38 represents the Annual number of nights with minimum temperature less than 74°F, the10th percentile of the data record at the Francisco C. Ada Saipan International Airport from 2006 to 2020. There were zero nights with minimum temperatures below 74°F in 2020. Original figures by Abby Frazier, using data from the NOAA GHCN-Daily database. (Grecni, Z., 2021).

Reference (Grezni, Z., 2021). States that the average air temperature, measured at Andersen Air Force Base from 1953 to 2002 (Figure 39) and Saipan's airport from 2006 to 2020 (Figure 40), has risen overall. No future projections downscaled to the island level are currently available for the CNMI. Average daily temperatures in Guam are projected to rise by 2.7–3.6°F under a low warming scenario and by 5.4–6.3°F under a high scenario by 2080–2099. Model projections for Guam indicate hot days over 90°F may increase to 257 days per year under a high scenario by the end of this century. In other words, more than 70% of days in the year are expected to see temperatures over 90°F.

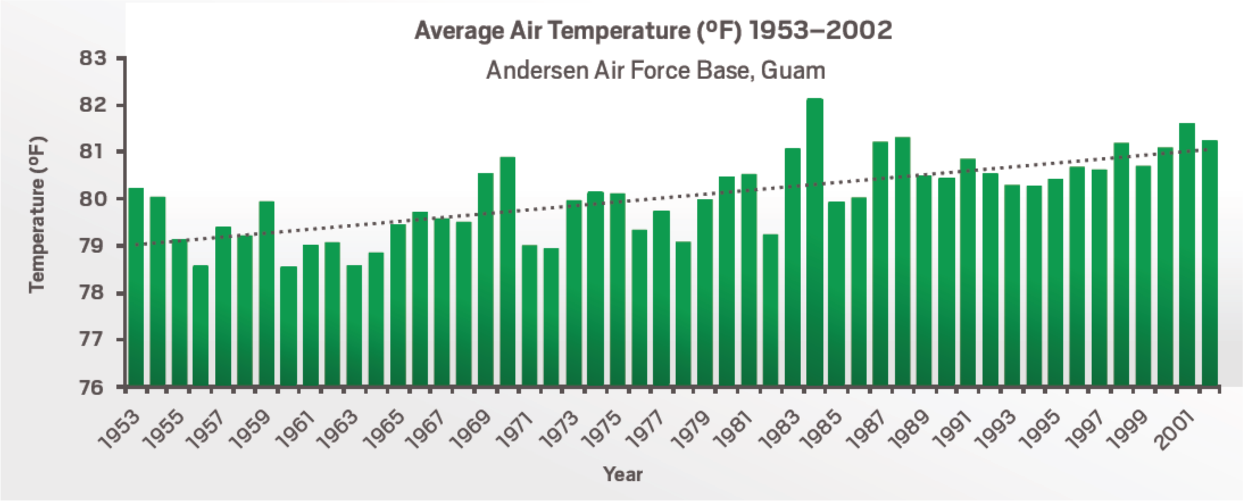

Figure 39. Average Air Temperature (1953-2002) Anderson AFB.

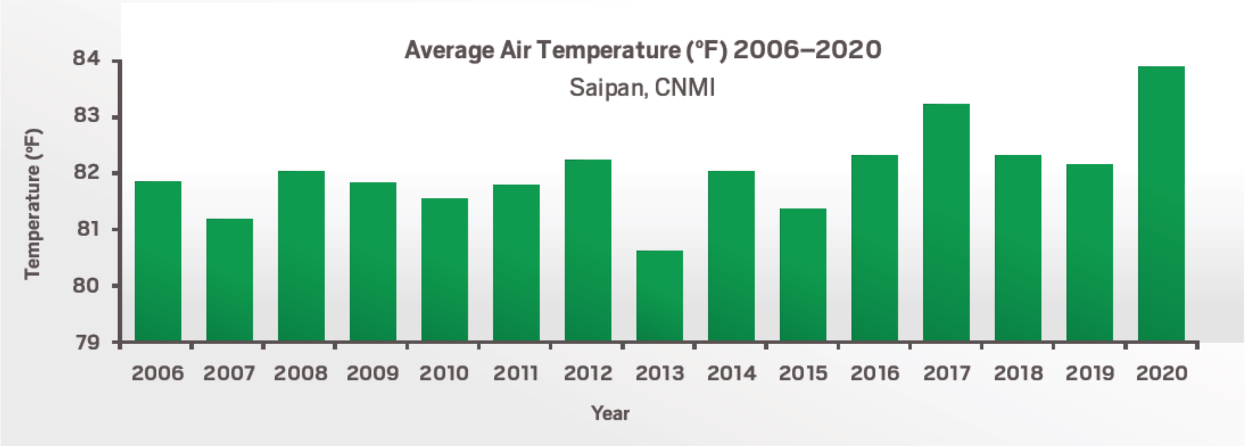

Figure 40. Average Air Temperature (2006-2020) Saipan

Note: Figure 39 illustrates the average annual air temperature at Andersen Air Force Base in Guam 1953–2002. The long-term linear trend indicated by the black, dotted line shows an increase over time. Figure 40 illustrates the Average annual air temperature from 2006 to 2020 at the Francisco C. Ada Saipan International Airport in the CNMI. Original figures by Abby Frazier, using data from the NOAA GHCN-Daily database. (Grecni, Z., 2021).

3.6 Precipitation

Reference (Grezni, Z., 2021). States on islands, rainfall is the primary source of all fresh water, making it essential to human communities and ecosystems. Rainfall patterns across the Marianas region are strongly linked to monsoons of the Eastern Hemisphere and the El Niño–Southern Oscillation (ENSO). As a result, annual rainfall is highly variable. Precipitation records in the CNMI contain significant gaps and are not representative of the geography of the islands. Thus, CNMI rainfall data is inadequate for climate studies. The nearest station with sufficient data, and thus considered the best available record relevant to the CNMI, is at Andersen Air Force Base in Guam. Rainfall patterns are consistent between Saipan and Guam, which can be attributed to both locations reacting similarly to ENSO (Figure 41). Thus, Guam's long-term rainfall record can be used to make inferences about the character of rainfall in the southern islands of the CNMI, including Saipan, Tinian, and Rota. At Andersen Air Force Base, the driest year recorded was 1998, during a strong El Niño, when rainfall was more than 39 inches below normal. The wettest year was 1976, when the station recorded more than 49 inches of above-normal rainfall.

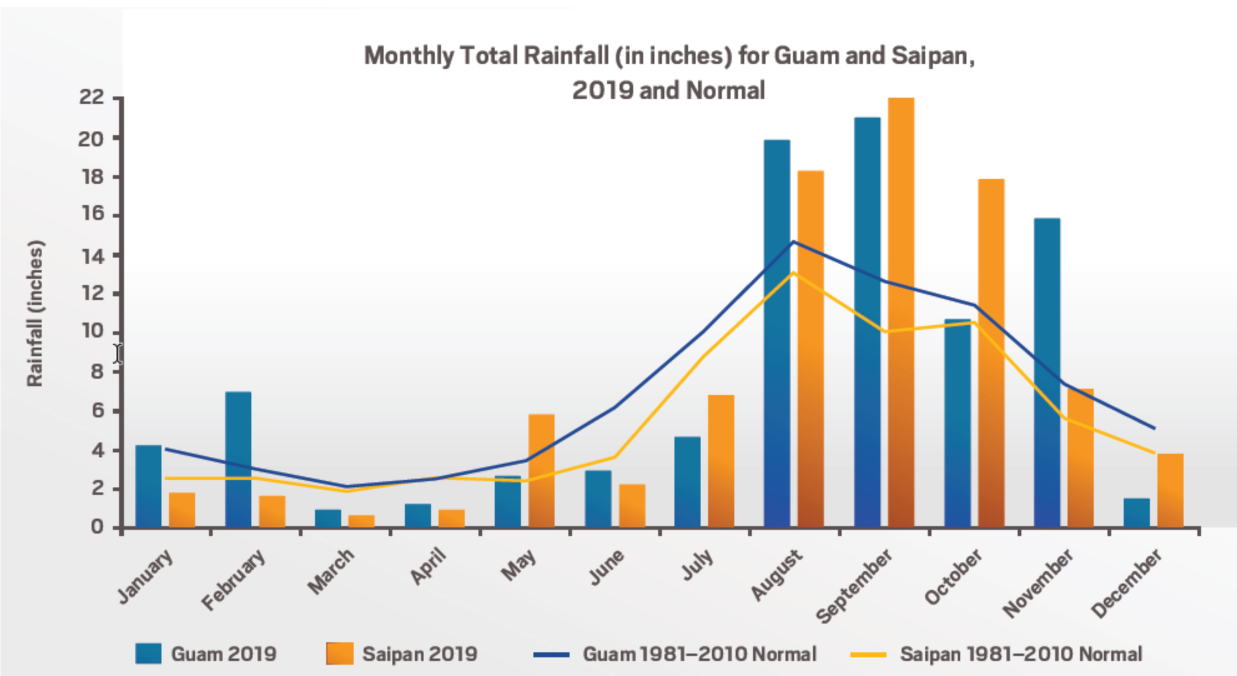

Figure 41. Monthly Total Rainfall for Guam and Saipan 2019 and Normal

Note: Figure 41 represents monthly rainfall totals at Guam's international airport (blue) and Saipan's international airport (yellow) in 2019 (bars) and a normal year (lines). During an El Niño, including the 2018–2019 event, rainfall responds similarly in Guam and Saipan, with a drier-than-normal first half of the year following the onset of El Niño. Figure from (Grecni, Z., 2021).

Reference Grezni, Z., 2021states that annual total rainfall at Saipan's airport from1989 to 2020 shows little change on average over 30 years and high year-to-year variability. This agrees with annual rainfall at Andersen Air Force Base (a proxy for CNMI rainfall), which is near the long-term normal value and shows no statistically significant change from the 1950s to present Global climate models project a 10–20% increase in average annual precipitation for the area of the Pacific including the CNMI by the end of the 21st century under the high scenario relative to 1986–2005. Under the low scenario, future change in annual rainfall is projected to range from no change to a 10% increase on average by the end of the century (IPCC 2013b). However, it should be noted that a subset of models downscaled to the island level for Guam project an average decrease in annual rainfall (7% overall) under the higher scenario for late this century relative to 1990–2009 The projections for Guam indicate reduced wet season rainfall (July to December), while dry season rainfall (January to June) is projected to increase slightly. The frequency of extreme rainfall at Saipan's airport (Figure 42) and Andersen Air Force Base has changed little on average over the length of the records (since 1989 and the 1950s, respectively). The annual number of extreme rainfall days from 1994 to 2020 at the Benjamin Taisacan Manglona International Airport on Rota is shown in Figure 43. Variability in the monsoon and other factors means rainfall is much greater in some years than others. In the future, the Marianas region is expected to experience more frequent and intense extreme rainfall events with global. Increased heavy rainfall events will result in increased runoff and increased potential for flooding and erosion.

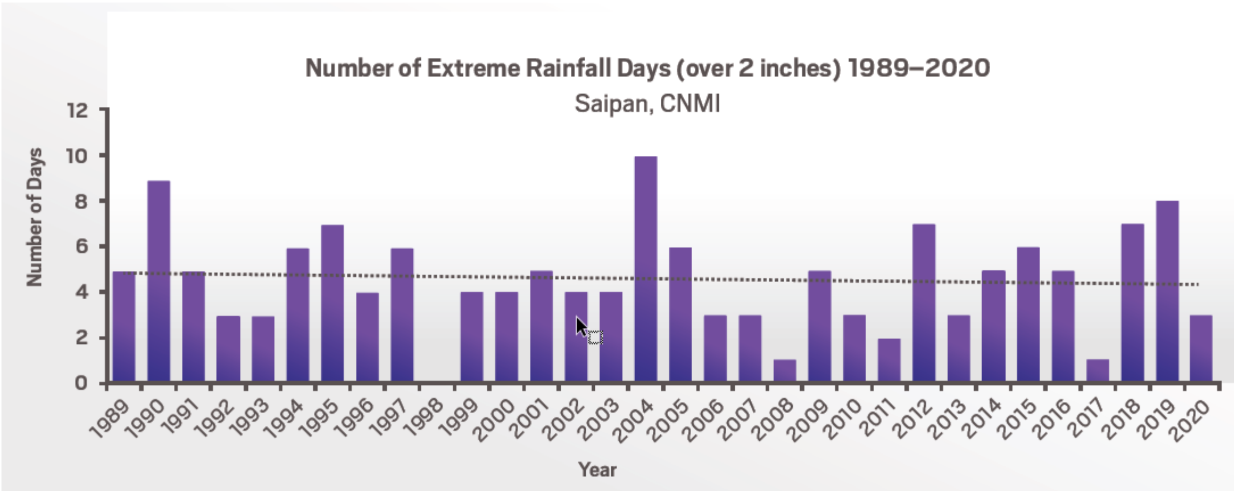

Figure 42. Number of Extreme Rainfall Days (Over 2 inches) 1989-2020 Saipan, CNMI

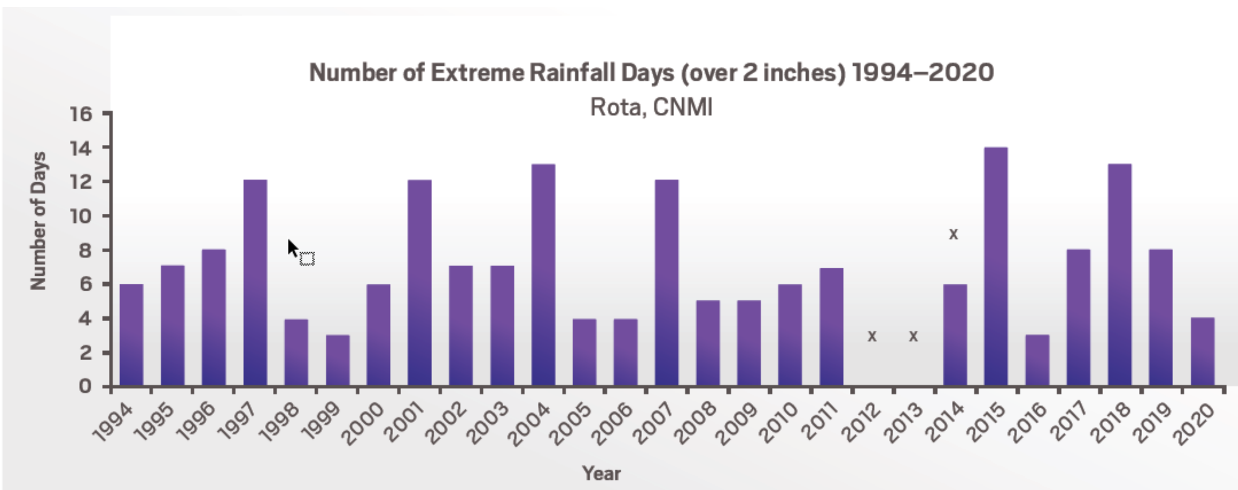

Figure 43. Number of Extreme Rainfall Days (over 2 Inches) 1994-2020 Rota, CNMI

Note: Figure 42 illustrates the annual number of extreme rainfall days, with daily rainfall totals exceeding the 99th percentile of the distribution (approximately 2 inches, or 51 mm) from 1989 to 2020 at the Francisco C. Ada Saipan International Airport. The linear trend line (black, dotted line) shows no significant change over the record. Figure 43 illustrates the annual number of days with daily rainfall totals exceeding 2 inches (51 mm) from 1994 to 2020 at Rota's international airport. The asterisks (*) represent yea rs in which significant data were missing. Original figures by Abby Frazier, using data from the NOAA GHCN-Daily database. (Grecni, Z., 2021).

Currently, future projections for drought frequency and intensity are not available for the CNMI. However, it is noteworthy that since 2015 the National Weather Service (NWS) has issued drought information statements for the Marianas for below-normal rainfall in every year except 2018. The frequency of days with no rainfall at Saipan's international airport (Figure 44) was above average in recent years. In the first half of 2020, the Marianas experienced exceptional drought.

Saipan's international airport had the second driest January–May on record in 2020. Downscaled climate projections for nearby Guam indicate drought conditions (defined here as more than 20% below mean annual historic rainfall) are projected to occur in 4 out of 10 years on average in 2080–2099 under the high scenario. This is an increase from the historic rate of 1.6 years out of 10 years on average (Gingerich et al. 2019; Zhang et al. 2016).

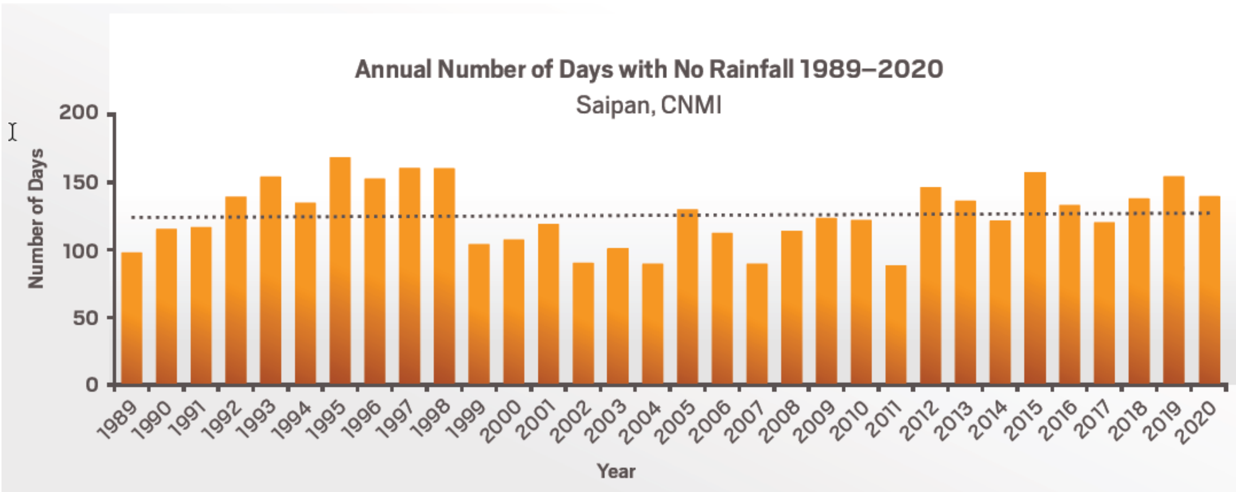

Figure 44. Annual Number of Days with No Rainfall 1989-2020 Saipan, CNMI

Note: Figure 44 illustrates Annual number of days with no rainfall from 1989 to 2020 at Saipan's international airport, CNMI. The black, dotted trend line shows no significant linear trend over time. Original figures by Abby Frazier, using data from the NOAA GHCN-Daily database. (Grecni, Z., 2021).

Based upon projected trends, mean temperatures, number of hot days, maximum temperatures, relative sea level change (RSLC), and rainfall intensity are projected to increase (NOAA NESDIS 142-8, 2013). The western North Pacific climate has experienced 60 years of increased temperatures with anticipated 1.1° F to 1.3° F increases in temperature by 2030, a 1.9° F to 2.6° F increase by 2055, and a 2.7° F to 5.1° F by 2090. Changes to mean annual rainfall are not projected to change significantly, however rainfall intensities and dry and wet extremes are projected to increase (NOAA[b] CNMI CRM, 2014).

3.7 Typhoons and Storms

Typhoons, tropical storms, and tropical depressions, referred to collectively as tropical cyclones, can bring intense winds, torrential rain, high waves, and storm surges to islands near their path. The effects of a tropical cyclone strike or near miss can severely impact lives and property. The Northern Mariana Islands lie within one of the most active regions in the world for tropical cyclones. A study covering 850 typhoons in the region found the intensity of the damaging storms has increased by about 10 per cent since the 1970s, according to climate scientists at the Scripps Institution of Oceanography at the University of California, San Diego. Using 20 models and a mid-range projection of carbon dioxide emissions, the researchers found the peak intensity of storms such as super Typhoon Haiyan, which transited through the Philippines in November 2013, are expected to become even stronger and more common. Such storms will be 14 per cent stronger by 2100, equivalent to adding another category to the current top severity rating of 5, the study found. (Hannam, 2015). Based on expected increases in El Niño events and typhoon intensity, existing flooding, and wind damage to coastal and island wide infrastructure will be exacerbated.

3.8 Relative Sea Level Change

Sea levels have risen gradually throughout the study area during the entire period of record. The nearest NOAA tidal Gage (Station ID: 1630000) is on the island of Guam, approximately 130 miles away. This gage is not USACE compliant to use for a sea level change analysis due to an apparent datum shift caused by a local earthquake in 1992. Recorded water levels from the Tanapag Harbor tide station (GLOSS ID 118) provide sufficient information to determine a rising sea level trend of 0.0072 ft/yr (2.2 mm/yr) over the 41 years of operations. Measurements pre-dating 1978 are not usable for sea level trend analysis. Tanapag Harbor water level trends are shown in Figure 45 (USACE, 2021).

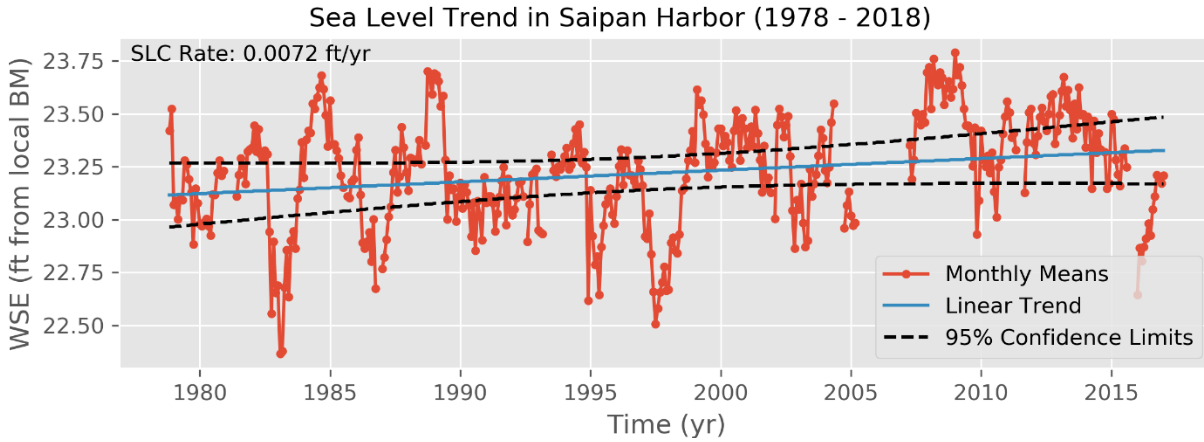

Figure 45. Sea Level Trends in Tanapag Harbor

In CNMI, eustatic water levels, tectonic activity and land subsidence all contribute to relative sea level change (RSLC). Figure 46 illustrates the low, intermediate, and high RSLC estimates based on the Tanapag Harbor gage (USACE, 2021). 1992 is the base year for calculations of sea level change in accordance with the established USACE methodology. It is noted that this 1992 year is based on tidal epoch and is unrelated to economic analysis. The extrapolated historic rate is represented by the blue line. The NRC Curves I and III predicted rates are represented by the green and red lines, respectively. The area shown in the highlighted box represents approximately a 100-year forecast period based on a 2022 base year. RSLC is anticipated to range between 0.9-7.0 feet by 2122. While not USACE policy, NOAA recommends use of the intermediate or high curves in planning, therefore incorporating a worst-case scenario for planning and accommodation for future high tide, storm surge, wave, and wave run up conditions. Sea level change for each island within CNMI are expected to be consistent with these estimates.

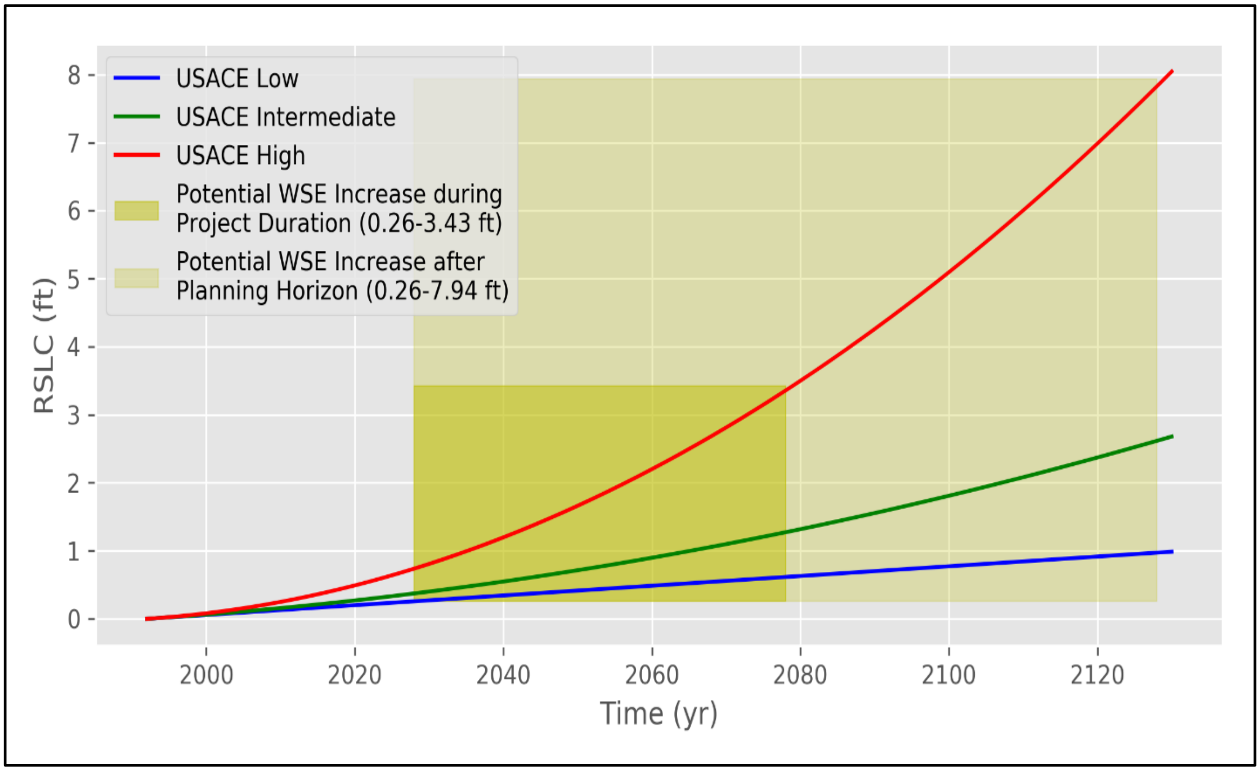

Figure 46. CNMI RSLC Projections

A projection of a three-foot RSLC by the year 2070 is consequential. Expectations of rainfall and typhoon intensification, as noted by the IPCC and NOAA, will threaten a presently vulnerable population.

The western island shoreline of Saipan between Tanapag Harbor and Susupe, which includes the city of Garapan, CUC power plant, and the American Memorial Park, is an area of concern for impacts from tropical storms and typhoons. It is categorized as the most vulnerable area in Saipan for RSLC and coastal erosion according to the Climate Assessment (NOAA[a] CNMI CRM, 2014). These areas contain low lying critical infrastructure (high school, government businesses, groceries, fuel, military facilities), residential communities and public businesses/hotels. Beach Road is a major throughway that is susceptible to flooding and RSLC along the western shore. A coastal storm risk management study by the USACE-Honolulu District is underway at the time of this writing (USACE, 2021).

Tinian Harbor, located on the island's southwest coastline, and the adjacent city of San Jose are vulnerable to RSLC and coastal flooding. The harbor is the only major port and serves a vital military function. The Marpo wetland is another critical resource related to drought vulnerability. The wetland is recharged by rainfall and is the sole source of drinking water for the island.

Rota has two harbors, on the west (Port of Rota) and east side (Mobile Marine Islands Inc.) on the Songsong peninsula. The eastern harbor is the sole import facility for the islands fuel source, which is petroleum used for power generation and transportation. A prior Rota harbor coastal management study was terminated.

Studies by NOAA suggest the future frequency of cyclones may decrease or stay the same, however the IPCC, NOAA, and others agree that future cyclones will bring greater rainfall, wind speeds, with assumed greater wind wave and flood damages.

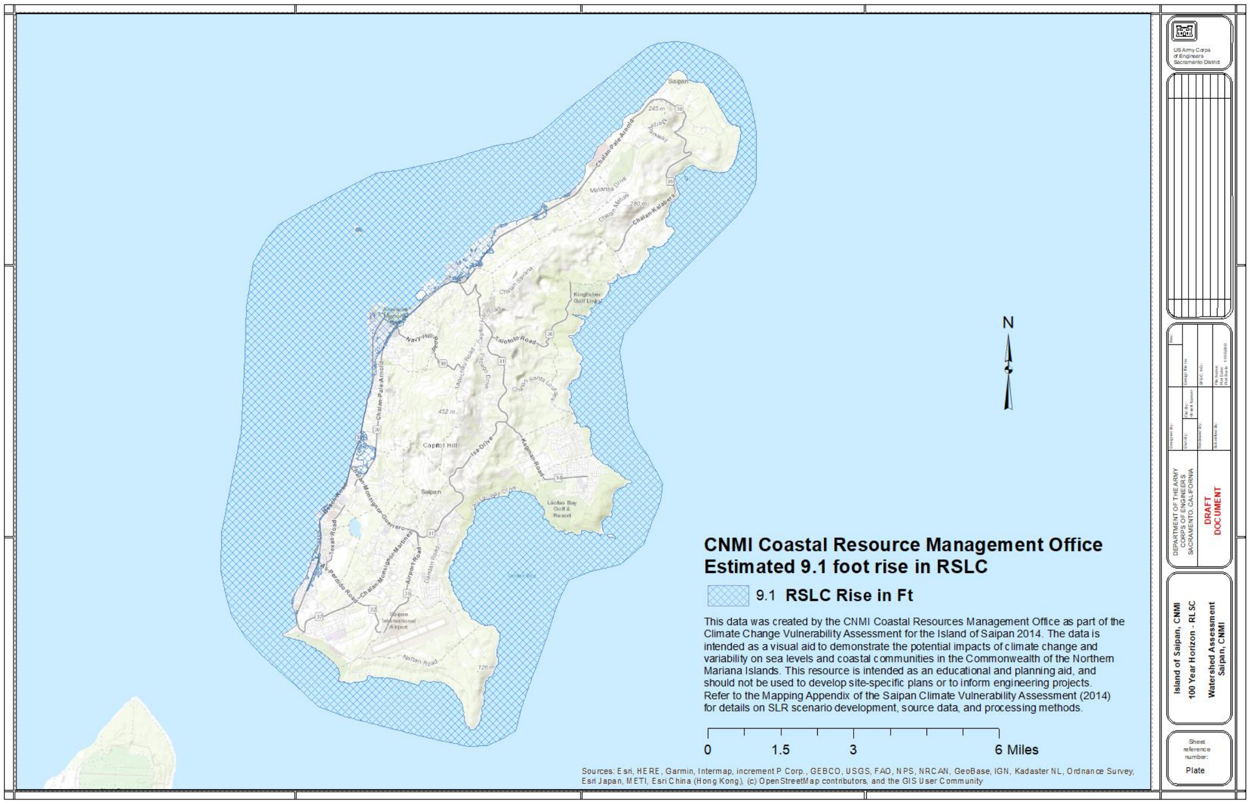

Figure 47. Estimated RLSC Inundation for Saipan (Year horizon 2120)

Coastal inundation can result from a variety of scenarios that occur at varying temporal scales. While long-term RSLC caused by climate change has the potential to impact Pacific Islands with varying severity, the combination of extreme events (storms, king tides, etc.) and long-term SLR will have more damaging and widespread effects. The mapping approach taken in the 2014 Climate Change Vulnerability Assessment for the Island of Saipan, CNMI VA acknowledges this range of coastal flooding threats, and attempted to integrate a variety of scenarios that represent them. The scenario presented in Figure 47 represents the historic maximum sea level estimate for 100-Year recurrence on Saipan, plus 50-year sea level rise projection (2067) based on NOAA 2017 High curve with a value of 9.1 feet. For year horizon 2120, Figure 46 estimates a -RSLC only- rise to be approximately 7.2 feet. The graphic above reasonably illustrates the potential impact to the inundation of Saipan from SLC in 100 years.

Figure 48 through Figure 52 represent the FEMA 1% AEP coastal flood hazard zones under future conditions. The high curve value from the USACE RSLC (of 2.8 ft by year 2070) was added to existing FEMA inundation maps for an approximation of expected impacts due to SLR. It is noted that NOAA SLR depth rasters are limited to integer SLR values, so a NOAA depth raster of three feet was used (for the 2.8-foot RSLC value). Therefore, the inundation projection is closer to the year 2075 than 2070. Additionally, FEMA does not archive depth maps from their FIS studies, only inundation polygons. To create depth maps from inundation polygons would require hydraulic modeling across the three CNMI islands which is outside the scope of the watershed assessment. To accommodate the task, coastal cross sections were automated in GIS. The cross sections were spaced every 100 feet and started at mean sea level (MSL) and terminated at the inundation boundary (running perpendicular to the shoreline). The local CNMI datum and MSL are essentially the same. The GIS method produces coarse results such as discontinuities between the cross sections, however, the depth maps are appropriate for the purpose of planning. The discontinuities appear as bands, and while they appear abrupt (near Garapan shoreline in central Saipan), the difference is on the order of 0.8-1.0 feet. Depths are relative to the local CNMI datum, which is equal to MSL.

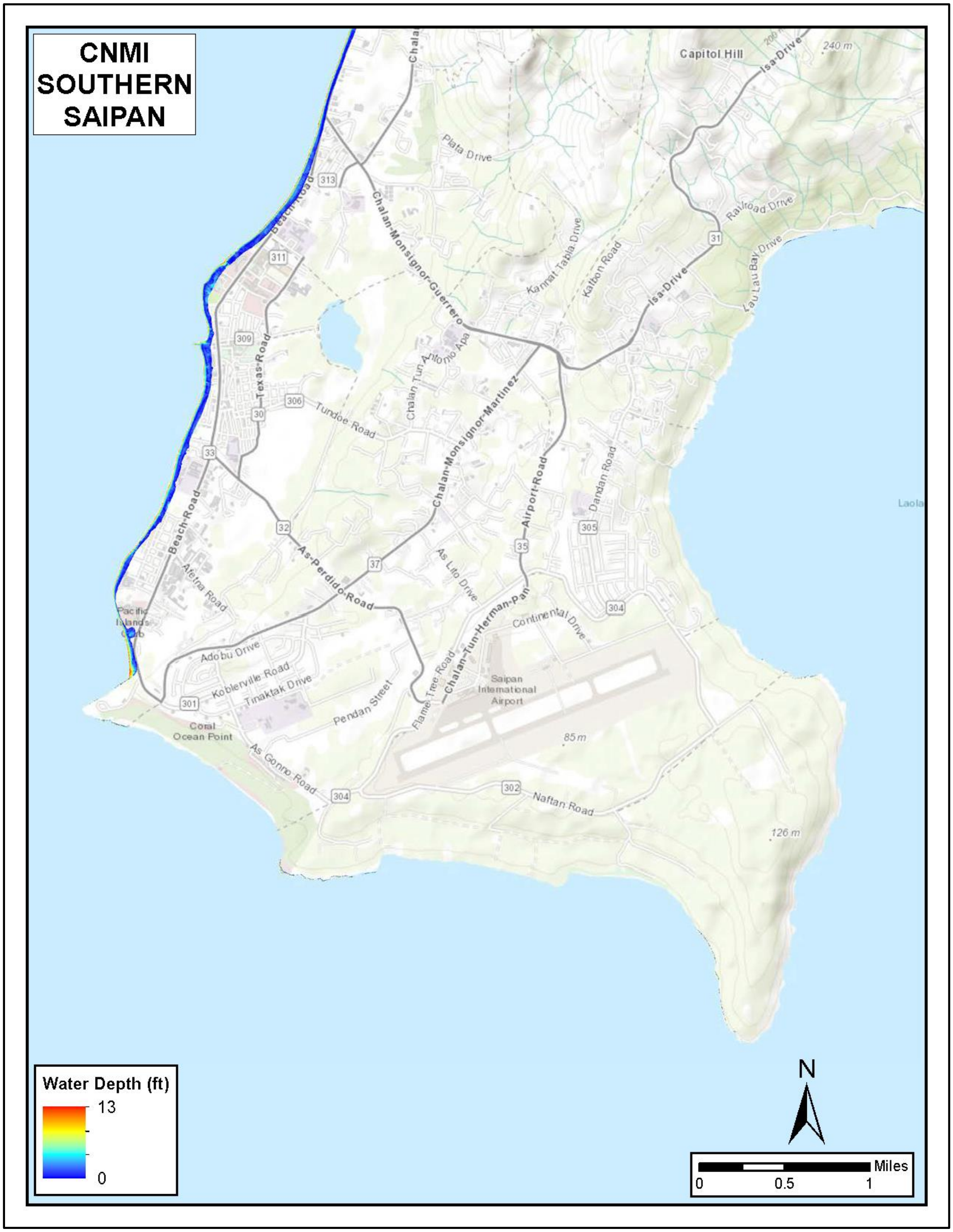

Figure 48. Southern Saipan, 1% AEP Coastal Flooding, Future Conditions

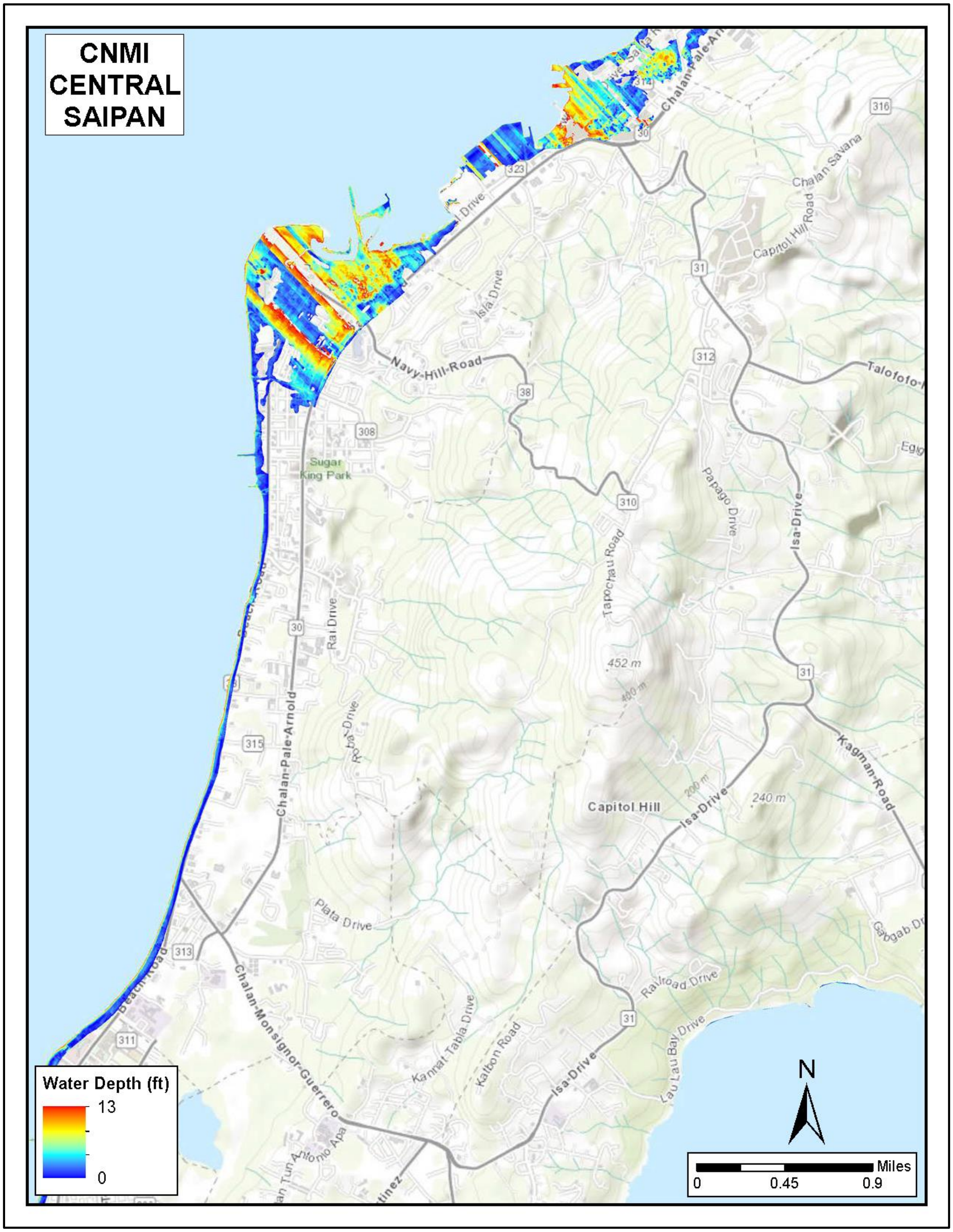

Figure 49. Central Saipan, 1% AEP Coastal Flooding, Future Conditions

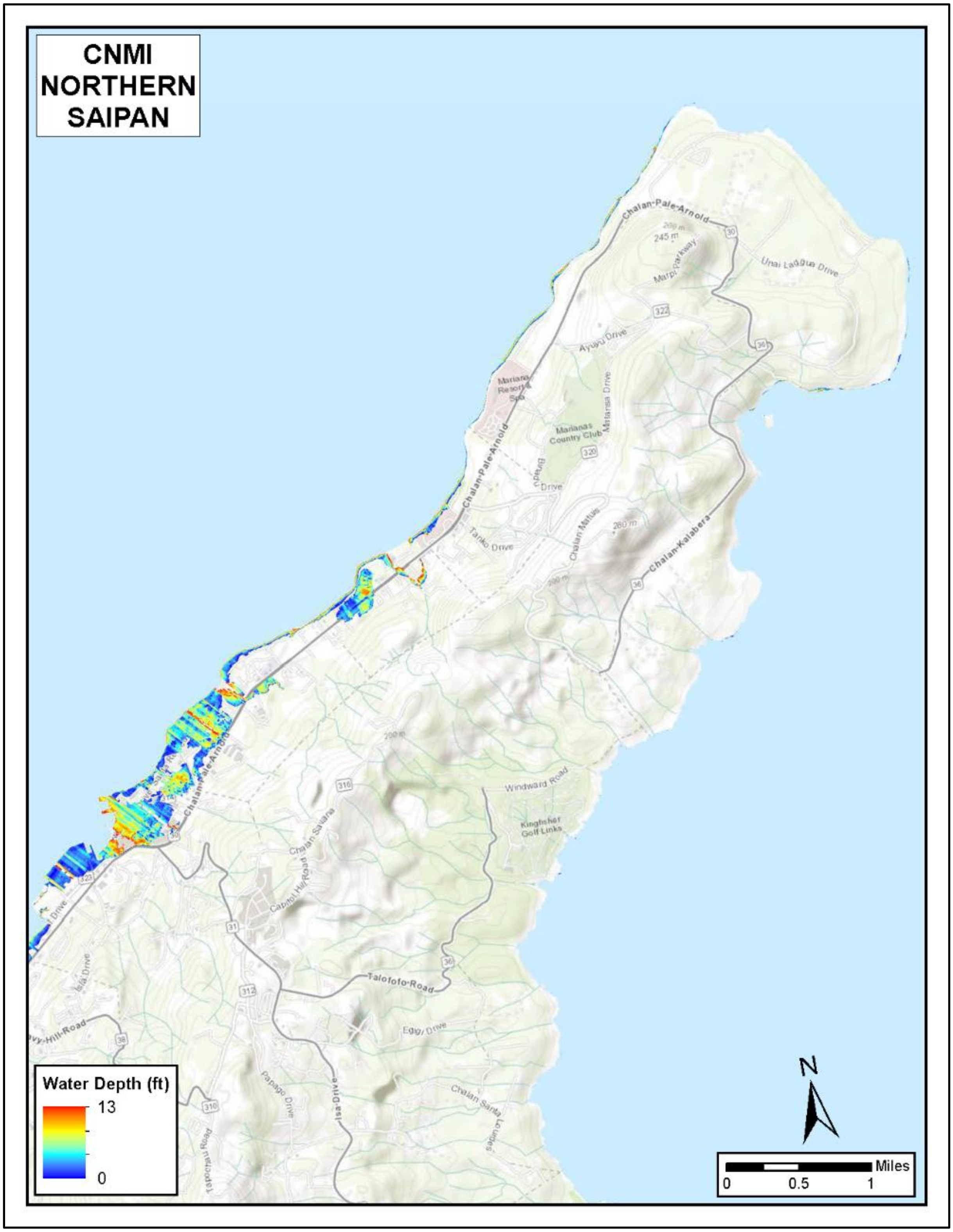

Figure 50. Northern Saipan,1% AEP Coastal Flooding, Future Conditions

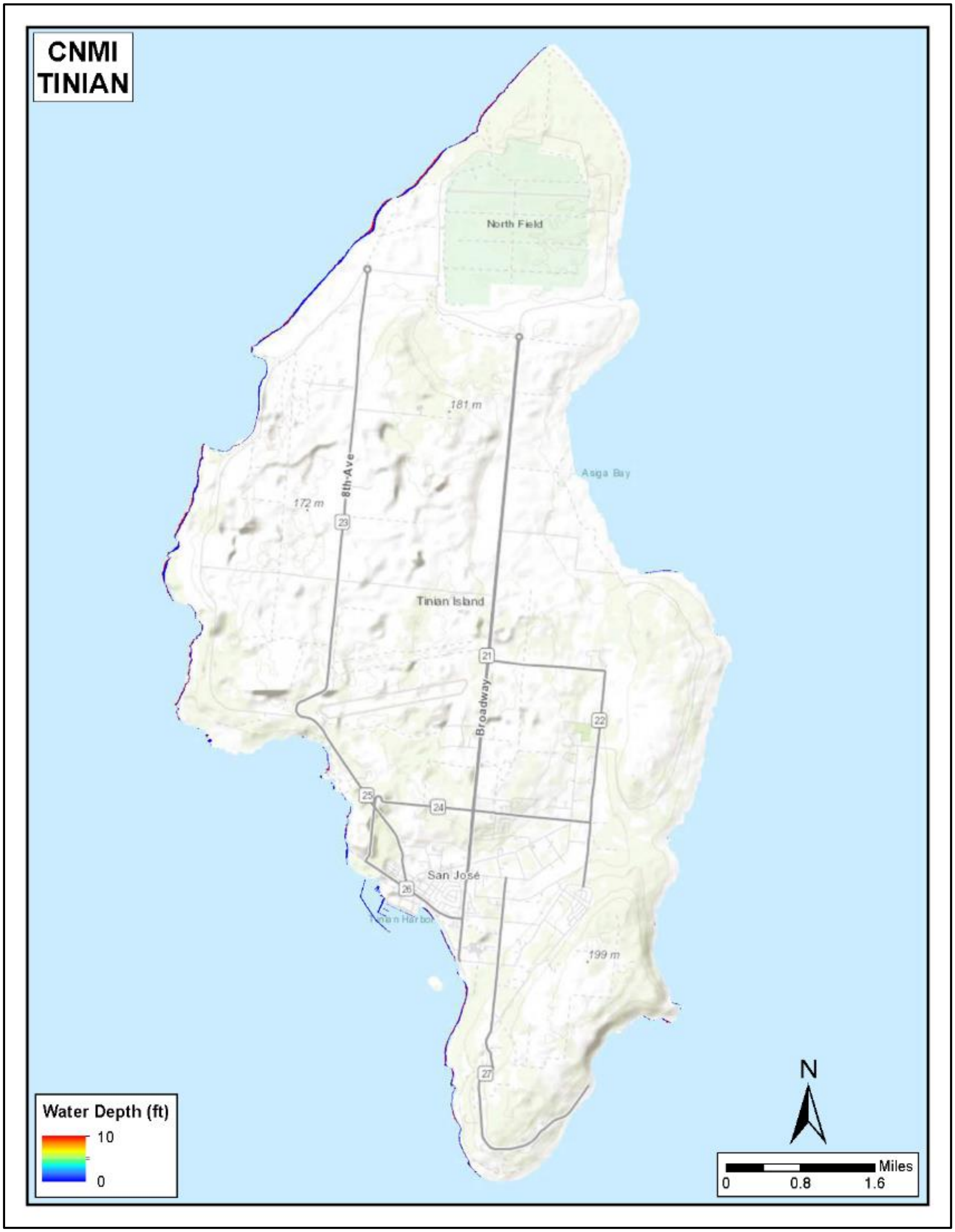

Figure 51. Tinian 1% AEP Coastal Flooding, Future Conditions

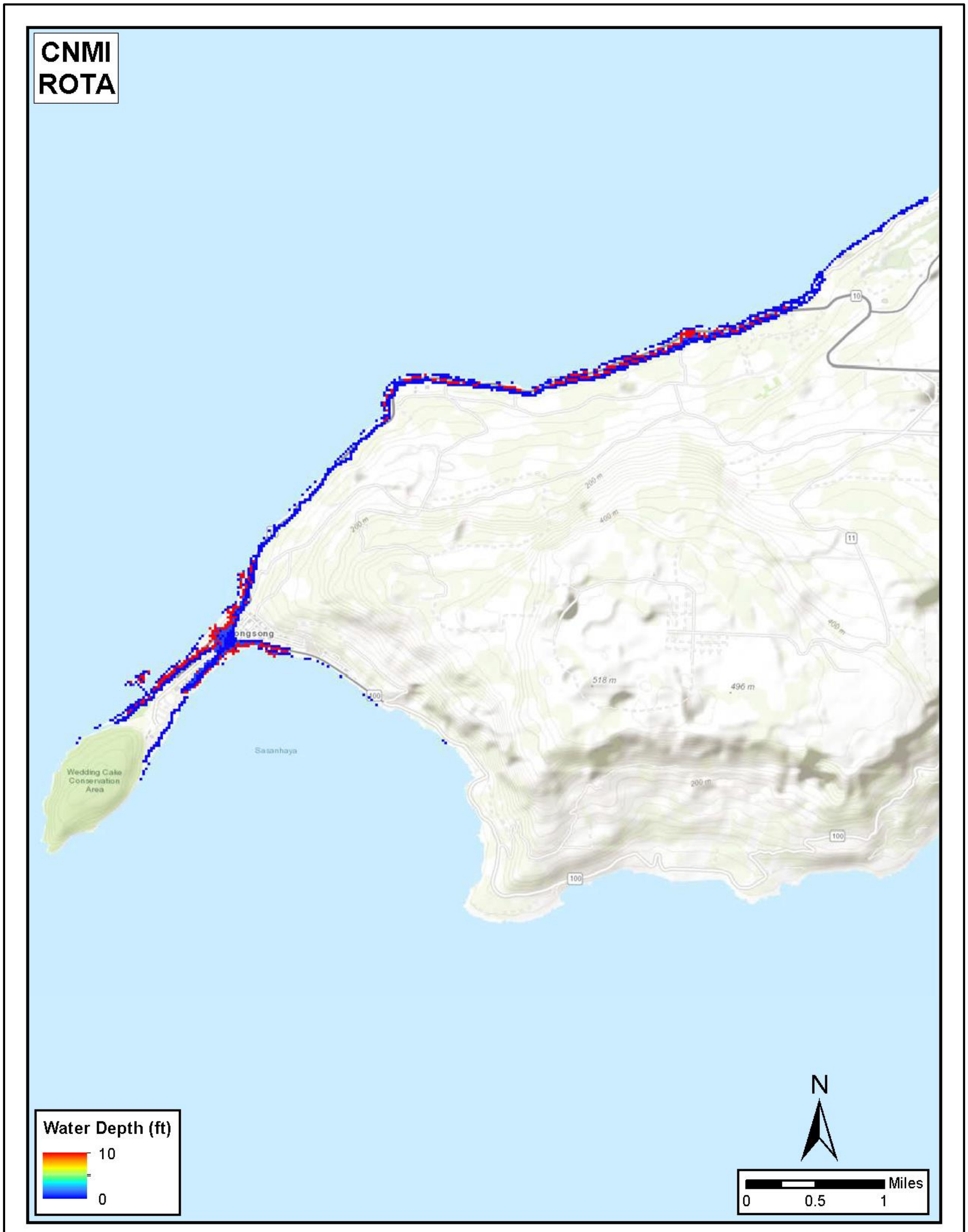

Figure 52. Rota 1% AEP Coastal Flooding, Future Conditions

3.9 Assessment of Climate Change Impacts to Inland Hydrology

The focus of the inland hydrology assessment is the flood risk management business line and the high flow regime. Large-scale floods can instigate streambank erosion and are critical to any future project performance. Consequently, the focus of the first order statistical analysis conducted as part of this assessment is on peak flow. Observed data is analyzed using the annual instantaneous peak flow records on the Island. Projected, future streamflow data cannot be visualized using the Vulnerability Assessment Tool as these products have only been developed for Hydrologic Unit Codes (HUC)'s within the Continental US.

3.10 Riverine and Urban Flooding

Population increase (Tinian Air Force base build up) and climate projections brings added stress from drought and rainfall extremes. Residential developments along Saipan's west coast (Achugao watershed thru Lower Base and western Susupe Lake) are highly developed and vulnerable to estuarine and coastal flooding. If rainfall intensification reaches the IPCC proposed 10-15% increase by the end of the century (IPCC-AR5 2014), urban flooding and storm water systems will be stressed beyond present vulnerable levels. Rainfall intensification drives increasing erosion rates and near shore pollution, reef, and fish mortality. Competition between development and ecosystem sustainability requires pre-emptive planning. Adding impervious developments along rivers and coastal shorelines under conditions of SLR and increased urban flooding requires mitigation and "no-regrets" plan formulation.

3.11 Riverine Erosion

Climate change, as discussed above, is expected to magnify weather extremes of droughts and intense rainfall and typhoons. Higher temperatures and droughts bring mortality to native grasses, wildlife, and forests. Native vegetation has evolved to grow in acidic volcanic soil regions. When this balance is disrupted, native plants that mitigate erosion and provide canopy are absent. Soils become drier and erodibility increases in response. Warmer climate and intensification of run off will increase sedimentation that's conveyed to lagoons, harbors, and near shore. Loss of vegetation and increased erodibility can lead to mudslides.

3.12 Tsunamis

Climate change is not expected to result in an appreciable (if any) increase in future tsunami vulnerability. Tsunami generation is not directly tied to measurable climate change. However, the low probability of tsunami hazards allows for a false sense of safety and complacency. Education, tabletop drills, signage, and preparation are critical. Tsunami wave amplitudes can be orders of magnitude higher than probable maximum hurricane waves and vulnerable residents need information for where safe zones are available. For low tsunami magnitude events, the predicted high curve for a 2.8-foot RSLC by 2070 means higher wave amplitudes and greater run up depths than those experienced under existing conditions. Climate change planning should consider safe zone re-evaluations from these RSLC impacts.

4 References

Carlson, E. and D. Doyle (2009). Development of Comprehensive Geodetic Vertical Datums for the United States Pacific Territories of American Samoa, Guam, and the Northern Marianas. Surveying and Land Information Science, Volume 69(1):5-17.

FEMA (April 2006), Flood Insurance Study, Commonwealth of the Northern Mariana Islands, Community Number 690000V000A

Fletcher, C.H., M. Barbee, M. Dyer, A. Genz, and S. Vitousek. 2007. Managaha Island shoreline stability assessment. Report to the Coastal Resources Management Office, Saipan, CNMI. 90p.

Grecni, Z., E.M. Derrington, R. Greene, W.Miles, and V. Keener, 2021: Climate Change in the Commonwealth of the Northern Mariana Islands: Indicators and Considerations for Key Sectors. Report for the Pacific Islands Regional Climate Assessment. Honulu, HI. East-West Center, https://eastwestcenter.org/PIRCA=CNMI

Greene, R. and R. Skeele. (2014) Climate Change Vulnerability Assessment for the Island of Saipan. Prepared for CNMI Office of the Governor - Division of Coastal Resources Management. Saipan: Commonwealth of the Northern Mariana Islands.

Hannam, Peter. 2015. Super typhoons to increase in strength with climate change, researchers find. The Sydney Morning Herald. https://www.smh.com.au/environment/climate-change/super-typhoons-to-increase-in-strength-with-climate-change-researchers-find-20150529-ghcbfs.html

Intergovernmental Panel on Climate Change (IPCC). IPCC-AR5 (2014), Fifth Assessment Report of the Intergovernmental Panel on Climate Change, Climate Change 2014 Synthesis Report.

International Panel of Climate Change, IPCC. 2019. Sea Level Rise and Implications for Low-Lying Islands, Coasts, and Communities, SROCC Chapter 4. Retrieved from https://www.ipcc.ch/srocc/download/

Marra, J. J., and M. C. Kruk, 2017: State of environmental conditions in Hawaii and the U.S. Affiliated Pacific Islands under a changing climate: 2017. NOAA National Centers for Environmental Information, 82 pp, https://statesummaries.ncics.org/ downloads/PI_State_of_the_Environment_2017.pdf.

National Oceanographic and Atmospheric Administration, National Weather Service (NOAA/NWS), NOWDATA (Tyan, Guam Weather Forecast Office), Data retrieved May 2021 from https://w2.weather.gov/climate/index.php?wfo=guam

National Oceanic and Atmospheric Administration (NOAA). 2018. Projected Response of Tropical Cyclone Intensity and Intensification in a Global Climate Model

National Oceanic and Atmospheric Administration (NOAA[a]) CNMI CRM (2014), Climate Change Vulnerability Assessment for the Island of Saipan

National Oceanic and Atmospheric Administration (NOAA[b]) CNMI CRM (2014), Climate Change Vulnerability Assessment for the islands of Rota and Tinian, CNMI

National Oceanic and Atmospheric Administration (NOAA[a]), NOAA OAR Special Report. 2013. Tsunami Hazard Assessment Special Series: Vol. 3, Tsunami Hazard Assessment of the Commonwealth of the Northern Mariana Islands.

National Oceanic and Atmospheric Administration (NOAA[b]) (2013), NOAA Technical Report NESDID 142-8, Regional Climate Trends and Scenarios for the US National Climate Assessment, Chapter 8, Climate of the Pacific Islands

National Oceanographic and Atmospheric Administration (NOAA[c]). 2013. Regional Climate Trends and Scenarios for the US National Climate Assessment Part 8 Climate of the Pacific Islands

National Oceanic and Atmospheric Administration (NOAA). NCEI (2021 online), Summary of Monthly Normals Saipan ITL MP. Retrieved from https://www.ncei.noaa.gov/access/services/data/v1?dataset=normals-monthly-1991-2020&stations=CQC00914855&format=pdf&dataTypes=MLY-TMAX-NORMAL,MLY-TMIN-NORMAL,MLY-TAVG-NORMAL,MLY-PRCP-NORMAL,MLY-SNOW-NORMAL

National Oceanic and Atmospheric Administration (NOAA). National Center for Environmental Data (NCEI), event data https://www.ncdc.noaa.gov/

National Oceanic and Atmospheric Administration (NOAA). NOAA Geophysical Fluid Dynamics Laboratory (2021), Global Warming and Hurricanes. Retrieved from https://www.gfdl.noaa.gov/global-warming-and-hurricanes/

National Oceanic and Atmospheric Administration (NOAA). NOAA/NWS, Climate Normals (Saipan, Guam Weather Forecast Office), Data retrieved May 2021 from http://xmacis.rcc-acis.org/

National Oceanographic and Atmospheric Administration (NOAA). Office of Coastal Management (OCM). Data retrieved April 2021 from https://tsunami.coast.noaa.gov/#/

National Oceanographic and Atmospheric Administration (NOAA). PMEL et al. (2010), with Joint Institute for Study of Atmosphere and Ocean University of Washington Seattle, Tsunami Hazard Assessment Special Series Vol. 1

National Oceanographic and Atmospheric Administration (NOAA). Atlas 14 (online). Data retrieved from https://hdsc.nws.noaa.gov/hdsc/pfds/pfds_map_cont.html?bkmrk=in

National Oceanographic and Atmospheric Administration (NOAA). 2013. Regional Climate Trends and Scenarios for the US National Climate Assessment, Part 8, Climate of the Pacific Islands

National Oceanographic and Atmospheric Administration (NOAA). Princeton University - Bhatia K. 2018. Projected Response of Tropical Cyclone Intensity and Intensification in a Global Climate Model

National Oceanographic and Atmospheric Administration (NOAA). 2019. El Niño and its Impacts on Guam and the Commonwealth of the Northern Mariana's Islands. Pacific ENSO Applications Climate Center.

National Oceanographic and Atmospheric Administration (NOAA, 2020). Global Historical Climatology Network Daily. NOAA Centers for Environmental Information accessed 5 April 2020, https://www.ncdn.noaa.gov/ghcn-daily-description.

Nurse, L.A., R.F. McLean, J. Agard, L.P. Briguglio, V. Duvat-Magnan, N. Pelesikoti, E. Tompkins, and A.Webb, 2014: Small islands. In: Climate Change 2014: Impacts, Adaptation, and Vulnerability. Part B: Regional Aspects. Contribution of Working Group II to the Fifth Assessment Report of the Intergovernmental Panel on Climate Change [Barros, V.R., C.B. Field, D.J. Dokken, M.D. Mastrandrea, K.J. Mach, T.E. Bilir, M. Chatterjee, K.L. Ebi, Y.O. Estrada, R.C. Genova, B. Girma, E.S. Kissel, A.N. Levy, S. MacCracken, P.R. Mastrandrea, and L.L.White (eds.)]. Cambridge University Press, Cambridge, United Kingdom and New York, NY, USA, pp. 1613-1654

Pacific Islands Regional Climate Assessment (PIRCA). 2022. www.pirca.org

Pacific Islands Regional Climate Assessment (PIRCA), Grecni, et al. 2021. Climate Change in the Commonwealth of the Northern Mariana Islands: Indicators and Considerations for Key Sectors. Retrieved May 2021 from https://www.eastwestcenter.org/publications/climate-change-in-the-commonwealth-the-northern-mariana-islands-indicators-and

U.S. Army Corps Engineers (USACE). May 2021. Saipan Beach Road Coastal Storm Risk Management Study, Draft Integrated Feasibility Report and Environmental Assessment, Appendix A

U.S. Army Corps Engineers (USACE). 2019. Sea-Level Change Curve Calculator (Version 2021.12). Retrieved April 2021 from https://cwbi-app.sec.usace.army.mil/rccslc/slcc_calc.html

U.S. Department of Agriculture (USDA). (online) gSSURGO soil survey. Retrieved June 2021 from https://gdg.sc.egov.usda.gov/GDGOrder.aspx

U.S. Department of Agriculture (USDA). (July 1989) Soil Survey of the Islands of Aguijan, Rota, Saipan, and Tinian Commonwealth of the Northern Mariana Islands

U.S. Geological Survey (USGS[b]). (Wood N.J. et al., 2019), Tsunami Warning and Preparedness: An Assessment of the U.S. Tsunami Program and the Nation's Preparedness Efforts.

U.S. Geological Survey (USGS). 2002. Geohydrology and Numerical Simulation of Alternative Pumping Distributions and the Effects of Drought on the Ground-Water Flow System of Tinian, Commonwealth of the Northern Mariana Islands, Report 02-4077

U.S. Geological Survey (USGS) Waterdata Talufofo Stream 16801000. Retrieved from https://nwis.waterdata.usgs.gov/usa/nwis/peak/?site_no=16801000